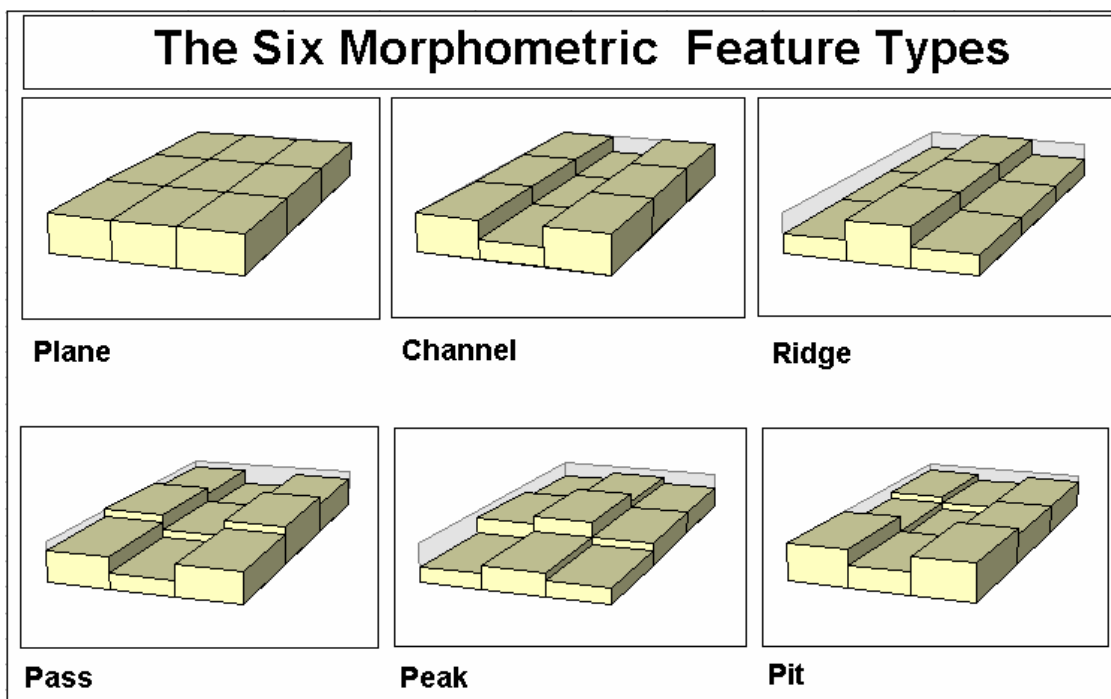


Chapter Five - Morphometric Characterisation

One of the overall aims of this study has been to develop a set of tools that describe the general geomorphometry of a surface. On the whole, this is quite distinct from the process of identifying specific geomorphometric features such as cirques or floodplains. There are however, a number of surface features that may be used both in the specific and general geomorphometric identification process. These features can be thought of as *morphometric* features rather than *geomorphometric* in that they are characteristic of any surface.

The most widely used set of morphometric characteristics, is the subdivision of all points on a surface into one of *pits*, *peaks*, *channels*, *ridges*, *passes* and *planes* (see Figure 5.1). The names of these features suggest a geomorphological interpretation, but they may be unambiguously described in terms of rates of change of three orthogonal components (see Table 5.1). Note that the components x and y are not necessarily parallel to the axes of the DEM, but are in the direction of maximum and minimum profile convexity.



Feature name	Derivative expression	Description
Peak	$\frac{\delta^2 z}{\delta x^2} > 0, \frac{\delta^2 z}{\delta y^2} > 0$	Point that lies on a local convexity in all directions (all neighbours lower).
Ridge	$\frac{\delta^2 z}{\delta x^2} > 0, \frac{\delta^2 z}{\delta y^2} = 0$	Point that lies on a local convexity that is orthogonal to a line with no convexity/concavity.
Pass	$\frac{\delta^2 z}{\delta x^2} > 0, \frac{\delta^2 z}{\delta y^2} < 0$	Point that lies on a local convexity that is orthogonal to a local concavity.
Plane	$\frac{\delta^2 z}{\delta x^2} = 0, \frac{\delta^2 z}{\delta y^2} = 0$	Points that do not lie on any surface concavity or convexity.
Channel	$\frac{\delta^2 z}{\delta x^2} < 0, \frac{\delta^2 z}{\delta y^2} = 0$	Point that lies in a local concavity that is orthogonal to a line with no concavity/convexity.
Pit	$\frac{\delta^2 z}{\delta x^2} < 0, \frac{\delta^2 z}{\delta y^2} < 0$	Point that lies in a local concavity in all directions (all neighbours higher).

Table 5.1 - Morphometric Features described by second derivatives.

The identification of these features forms the basis of the techniques described in this chapter for describing DEM characteristics. The first two sections describe how the features themselves may be identified. The third section extends the technique to extract multi-scale behaviour. The final section concentrates on the hydrological implications of the layout of these morphometric features. It is worth noting at this stage that this classification produces point-based categories (pits, passes, and peaks), two line-based categories (channels and ridges) and one area-based category (planes).

5.1 Feature Identification

The standard method of identifying morphometric features is to pass a local (usually 3 by 3) window over the DEM and examine the relationships between a central cell and its neighbours (eg. Peucker and Douglas, 1975; Evans, 1979). Alternative methods exist for terrain modelled with contour lines (eg. Maxwell, 1870; Tang, 1992), but will not be considered here. This section will consider how the multi-scaled parameterisation discussed in the previous chapter may be applied to morphometric feature identification.

5.1.1 Quadratic Approximation

For consistency with the general geomorphometric parameters identified previously, the second derivatives required to identify all six features are extracted using quadratic approximation of some local window (see section 4.4). Cross-sectional curvature (*crosc*) is used to characterise the second derivative as this is the convexity measure that is most closely related to geomorphological process. At locations with a non-zero slope, channels have a negative *crosc*, ridges a positive *crosc*, and (sloping) planes a *crosc* of zero. Additionally, we can measure the longitudinal curvature *longc* in order to define the three remaining feature types. Pits have a negative *crosc* and *longc*, peaks a positive *crosc* and *longc*, and passes *crosc* and *longc* with opposite signs.

For cases of zero slope, the slope direction (aspect), *crosc* and *longc* remain undefined. In such cases an alternative measure of convexity is required that is not based on slope direction. Young (1978) shows how the maximum and minimum convexity values can be derived from the quadratic coefficients *a*, *b* and *c* for this special case:

For a surface modelled by the quadratic,

$$z = ax^2 + by^2 + cxy + dx + ey + f$$

where gradient is zero ($d^2 = e^2 = 0$), maximum and minimum convexity values are,

$$\maxic = -a - b + \sqrt{(a - b)^2 + c^2}$$

$$\minic = -a - b - \sqrt{(a - b)^2 + c^2}$$

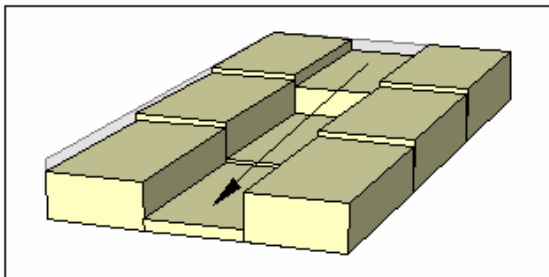
Together, *slope*, *crosc*, *longc*, *minic*, and *maxic* provide a complete and unique set of conditions for defining all six morphometric features (Table 5.2)

<i>Feature</i>	<i>slope</i>	<i>crosc</i>	<i>longc</i>	<i>maxic</i>	<i>minic</i>
Peak	0	#	#	+ve	+ve
	+ve	+ve	+ve	#	#
Ridge	0	#	#	+ve	0
	+ve	+ve	0	#	#
	+ve	0	+ve	#	#
Pass	0	#	#	+ve	-ve
	+ve	+ve	-ve	#	#
	+ve	-ve	+ve	#	#
Plane	0	#	#	0	0
	+ve	0	0	#	#
Channel	0	#	#	0	-ve
	+ve	-ve	0	#	#
	+ve	0	-ve	#	#
Pit	0	#	#	-ve	-ve
	+ve	-ve	-ve	#	#

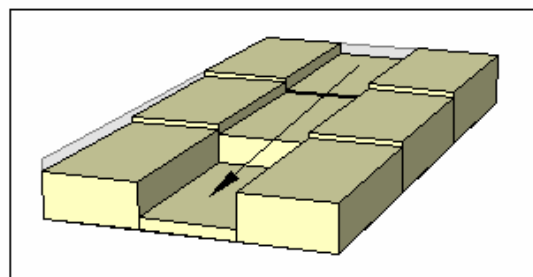
Table 5.2 Morphometric features defined by the sign of five morphometric parameters. # indicates undefined, or not part of selection criteria.

It becomes necessary to check longitudinal curvature when identifying ridges and channels where the ridge/channel sides are of significantly different heights. In such cases the slope direction is unlikely to be 'down-channel' (or along the ridge), but obliquely across the length of the feature. Additionally there is a possibility of misclassification for features similar to those illustrated in Figure 5.2. In Figure 5.2(a) the negative cross-sectional curvature (orthogonal to the slope vector represented by an arrow) suggests a channel, but the longitudinal curvature is also negative, forcing classification as a pit. Figure 5.2(b) shows a similar situation where a positive longitudinal curvature forces an apparent channel to be classified as a pass. The result of applying this classification algorithm to a real geomorphological surface is to overrepresent the numbers of point-based categories (peaks, passes and pits).

Two spurious feature classifications



(a) Apparent channel classified as a pit



(b) Apparent channel classified as a pass

A simplified and improved algorithm for classification is suggested here that preserves the continuity of line-based channels and ridges to a far greater extent. This provides an advantage over traditional methods of feature selection based on logical comparison of neighbours (eg, Peucker and Douglas, 1975; Jensen, 1985; Bennet, 1989; Skidmore, 1990).

It is assumed that all locations that have a local slope must be either planar, form part of a channel or form part of a ridge. Pits peaks and passes are assumed only to occur where local slope is zero. These assumptions are perhaps closer to our own models of the surface features. The anomalous classifications shown in Figure 5.2 are eliminated. The selection criteria are shown in Table 5.3.

<i>Feature</i>	<i>slope</i>	<i>crosc</i>	<i>maxic</i>	<i>minic</i>
Peak	0	#	+ve	+ve
Ridge	0	#	+ve	0
	+ve	+ve	#	#
Pass	0	#	+ve	-ve
Plane	0	#	0	0
	+ve	0	#	#
Channel	0	#	0	-ve
	+ve	-ve	#	#
Pit	0	#	-ve	-ve

Table 5.3 Simplified feature classification criteria.

These rules provide the basis for the morphometric classification considered in the rest of this chapter.

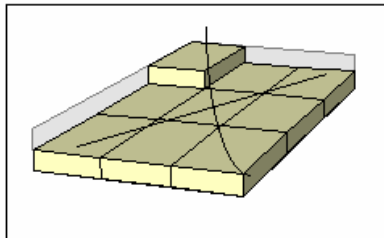
5.2 Slope and Curvature Tolerance

The method described above, if strictly applied will tend to produce surfaces that consist almost entirely of interdigitating channels and ridges. This is because (i) a quantised DEM will rarely

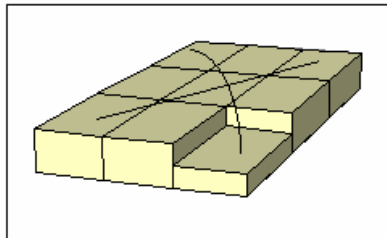
produce truly planar facets with profile convexity components of zero (the only relatively common exception being flat regions such as lakes and coastal areas), and (ii) true peaks, passes and pits usually have an overall slope value when their neighbours are considered. Figure 5.3 shows how small variations in one or two values can change the nature of the feature detected. To overcome this two tolerance values are introduced that account for (i) and (ii) above.

Let T_{convex} be the minimum *crosc* that represents a true cross-sectional convexity/concavity. In effect, this value defines the minimum concavity of a channel cross-section and convexity of drainage divides. Let T_{slope} be the minimum *slope* that represents a true slope. In effect, this value defines the minimum longitudinal channel or ridge slope in which local variations can occur, without breaking it up with a series of pits, passes and peaks. The values of these tolerances are somewhat arbitrary, yet it is necessary to have the flexibility to vary the feature selection process according to the nature of terrain. The algorithm representing these modified rules is shown in Algorithm 5.1 (coded as part of *r.param.scale* and *d.param.scale* in the Appendix). The results of varying the both tolerance values for a mountainous DEM are shown in Figure 5.4 as *small multiples* (Tufte, 1990). The position of each image within the figure indicates the magnitude of the two tolerance values.

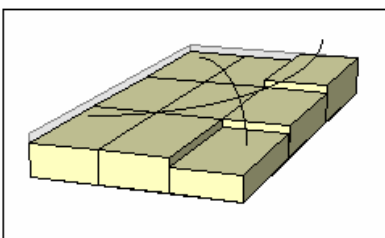
Five Spurious Morphometric Features



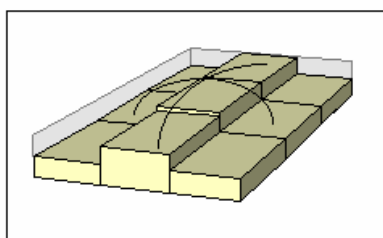
Channel



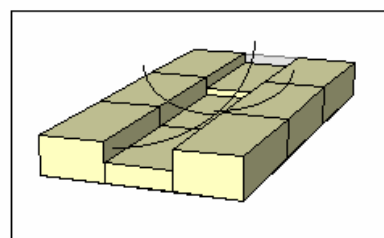
Ridge



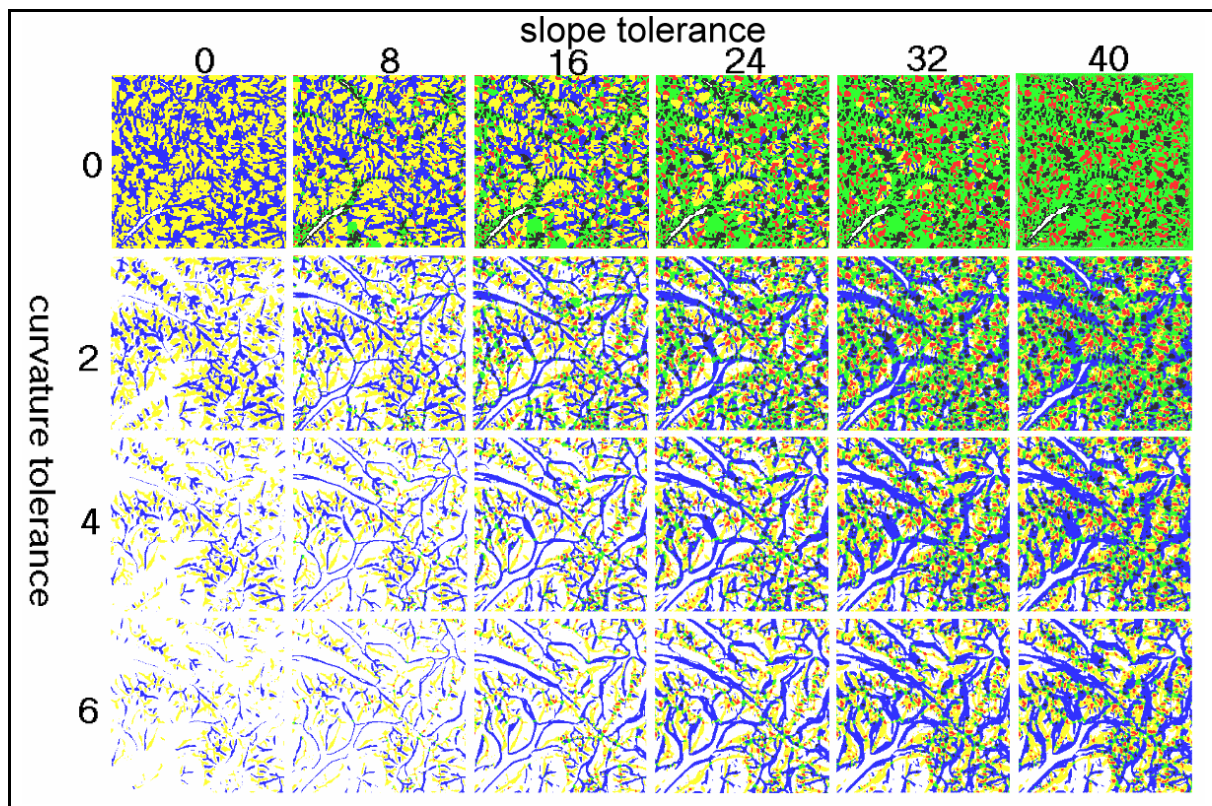
Pass



Peak



Pit



```

Synopsis: Mfeature defines a morphometric feature described by a bivariate quadratic function.
Parameters: coeff[6]      Array holding the 6 quadratic coefficients a to f
              n          Size of side of local window
Globals:   Tslope Minimum gradient that defines a non flat surface
              Tconvex Minimum convexity defining a non-planar surface
              g          Grid resolution of DEM
Locals :  slope       Maximum gradient
              crosc      Cross-sectional convexity
              minic,maxic Minimum and maximum convexity

```

```

Mfeature(coeff)
{
    /* Measure morphometric parameters */
    slope = atan(sqrt(d*d + e*e))
    crosc = n*g*(b*d*d + a*e*e - c*d*e) / (d*d + e*e)
    maxic = n*g*(-a-b+sqrt((a-b)*(a-b) + c*c))
    minic = n*g*(-a-b-sqrt((a-b)*(a-b) + c*c))

    /* Identify morphometric features */
    if (slope > Tslope)           /* Case 1: Surface is sloping */
    {
        if (crosc > Tconvex)
            return (RIDGE)
        if (crosc < -Tconvex)
            return (CHANNEL)
        else
            return (PLANAR)
    }
    /* Case 2: Surface is horizontal */
    if (maxic > Tconvex)
    {
        if (minic > Tconvex)
            return (PEAK)
        if (minic < -Tconvex)
            return (PASS)
        else
            return (RIDGE)
    }
    if (minic < -Tconvex)
    {
        if (maxic < -Tconvex)
            return (PIT)
        else
            return (CHANNEL)
    }
    return(PLANAR)
}

```

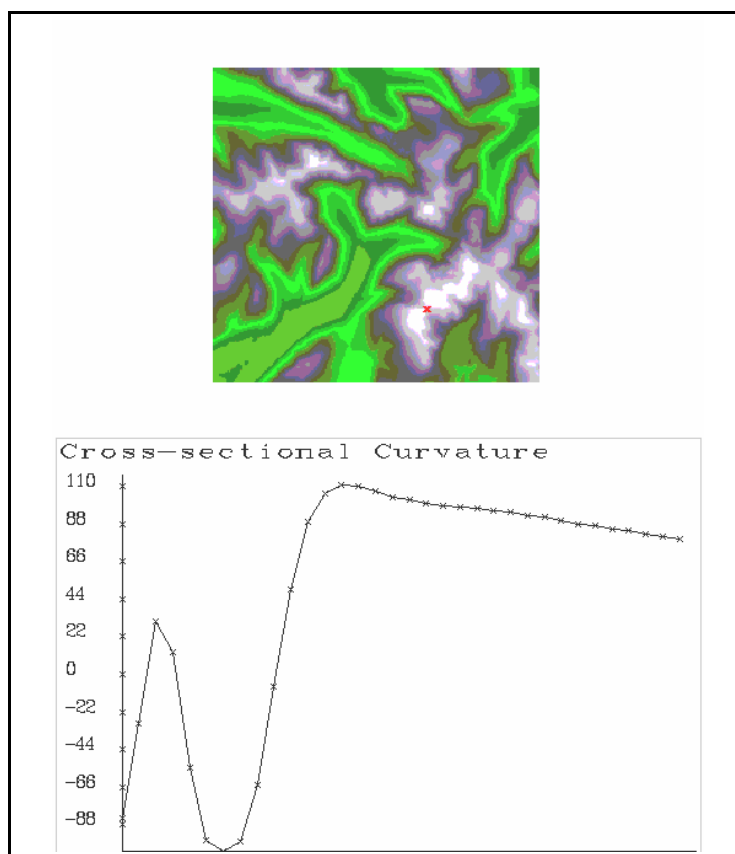
5.3 Multi-scale feature classification

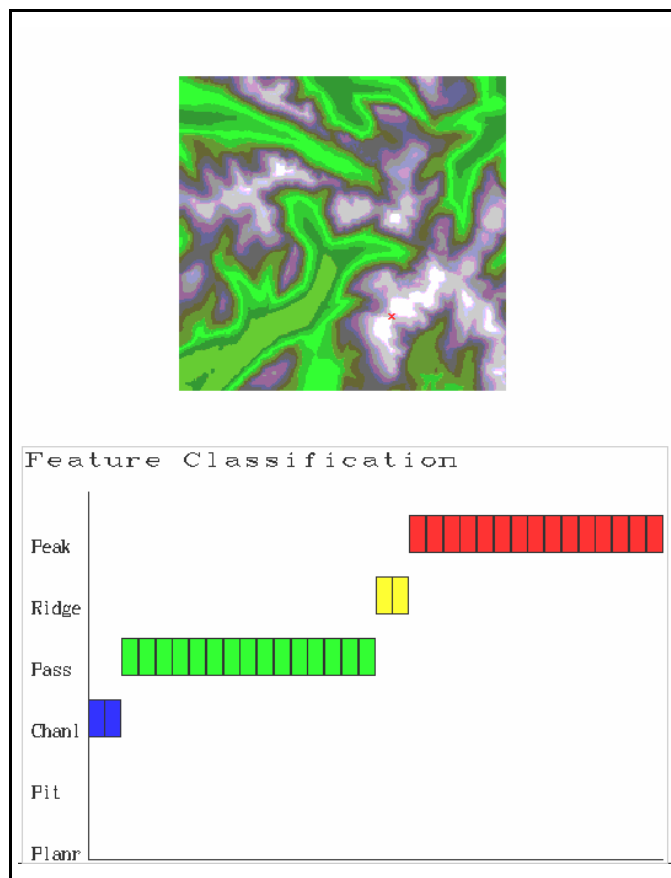
The argument presented in the previous chapter was that one resolution dependent parameterisation is not sufficient to describe surface form. Surface parameters should be able to be expressed at a variety of sizes. Likewise, a rule-based classification of morphometric features based on those parameters should also be multi-scale. If we are to match morphometric 'peaks' to our own geomorphometric understanding, it is very unlikely that the scale defined by the DEM resolution will be sufficient. Thus the rules for feature classification defined above are scale independent. The parameters $a-f$ in (1) can be found for any window size before being used for classification.

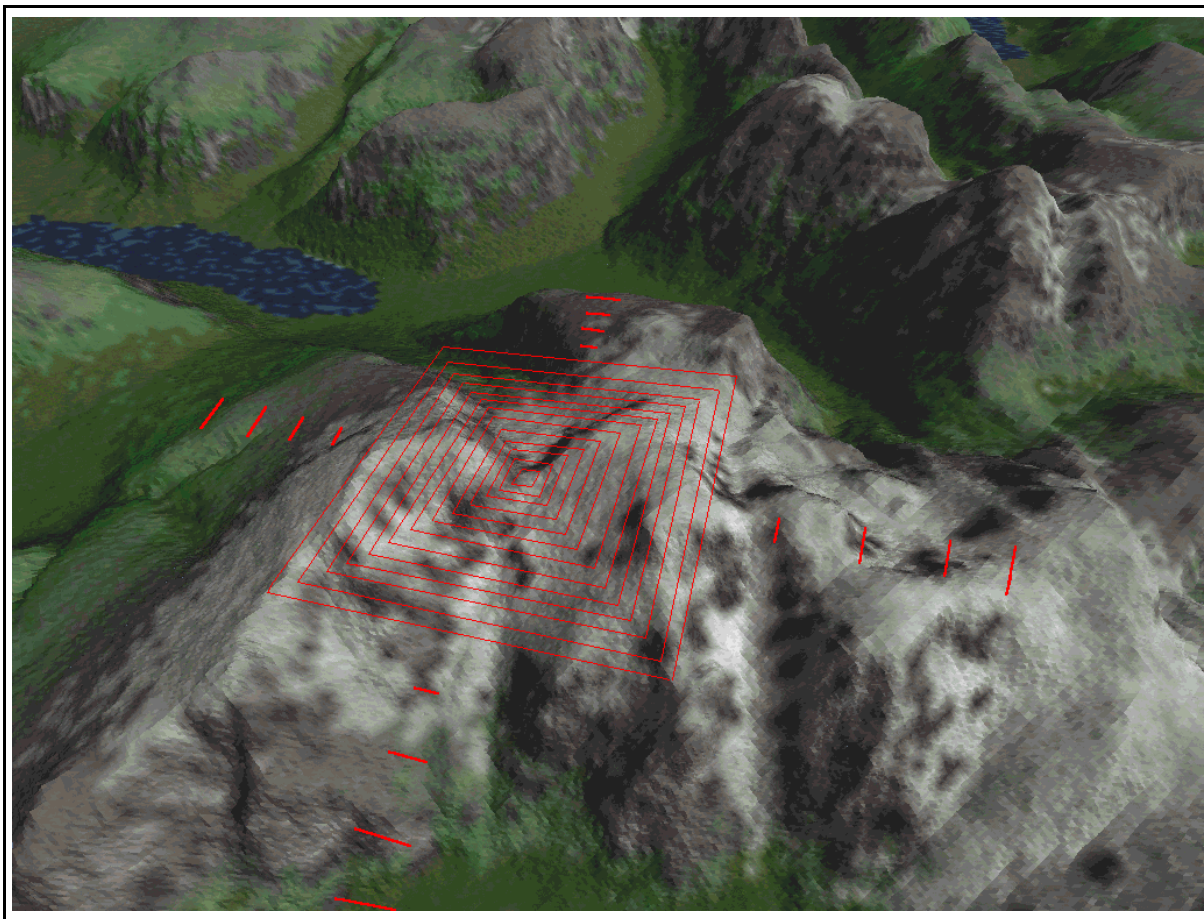
The result of applying a multi-scale approach is that each location has multiple feature attributes. These can be visualised in a number of ways. Animation may be used with 'time' representing change in spatial scale (an approach adopted by Wood *et al*, 1996 for characterising population density surfaces). Alternatively, small multiples may be used to show the 'slices' through this sequence (see Chapter 6 for examples of this). The third alternative that is adopted here for an interactive visualisation context, is the multi-scale 'probe'. A mouse is passed over a DEM so that when a mouse button is clicked, the feature classification of the relevant DEM cell is found over a range of window sizes. The result is a graphical representation of the *feature membership function*. Equally important is an equivalent representation of the morphometric parameters (*crosc* and *slope*) used for the classification. The C code for interactive probing in this way is shown in the Appendix (*d.param.scale*).

Figures 5.5 and 5.6 show an example of this probe applied to part of the Lake District DEM. The cross in the upper image of both figures indicates the point selected for query. In both cases this corresponds to Mickledore - a well known gap between England's two highest mountains, Scafell Pike (to the North East) and Scafell (to the South West). This location would probably be considered by most visitors to the location as a 'pass' with two steep gullies running orthogonally to the direction of the two peaks on either side. Yet if we are to classify the point location, the type of feature should (and does) depend on the scale of interest. The lower image

in both figures shows the relationship between the parameter or feature classification and local window size. The X-axis in both figures ranges from 3 x 3 cells at the origin to 69 x 69 cells at the right hand side. At the resolution of the DEM this corresponds to a spatial range of 150m to 3.5km. The extent of the kernel shown graphically in Figure 5.7 with kernels 3x3 to 29x29 shown as red squares, and kernel boundaries indicated for sizes 39x39, 49x49, 59x59 and 69x69.







Both cross-sectional curvature and feature type vary with scale. Short lags would indicate that the location is part of a convex channel. As the scale is widened, it is revealed that this channel lies within a larger pass, that itself is part of an extended convex ridge. The largest lags indicate a peak feature. It is suggested that this scale based progression of characteristics is much more useful than a single morphometric parameter or classification. It provides a landform *signature* (Pike, 1988) that is more discriminating than a single feature classification, but sufficiently general to be of use in an analytical context.

There are likely to be contexts when a single measure or classification is required, so it is useful to at least quantify the variability of measurements. For (the ratio scale) parameters, the mean and standard deviation are calculated. For the categorical feature classification, the mode and scaled entropy is calculated,

$$E = - \sum_{i=1}^n p(f_i) \cdot \log[p(f_i)]$$

$$E_{\max} = -\log(1/n)$$

$$E_s = \frac{E}{E_{\max}}$$

where $p(f_i)$ is the proportion of measurements classified as feature type i and n is the number of feature types (6 in this study).

This may be used to distinguish locations that are consistently classified as the same feature ($E_s = 0$) from locations that have a high degree of scale dependency in their classification ($E_s = 1$). While this form of interrogation is useful in an interactive visualisation context, it is difficult to identify the spatial pattern of entropy across the image. To visualise both the spatial distribution and scale dependency of measures it is necessary to create several raster layers containing morphometric feature classification at a range of scales. Using simple map algebra, these maps can be combined to produce two new images, one of the modal classification, the other of entropy (see Algorithm 5.2). Thus it is possible to produce a feature membership map and a classification uncertainty map. These may be combined into a single hue-intensity image (see Chapter 6).

```

# #Mapcalc script to calculate morphometric classification of morphometric
#
# Note: feat9, feat15, feat21 etc. are the map layers containing feature
# classification at the corresponding kernel sizes.
# pplne,ppit,pchan etc. contain the proportion of maps classified
# in each feature category.

r.mapcalc << EOF

pplne =      (feat9 ==0) + (feat15==0) + (feat21 == 0) +
              (feat27 == 0) + (feat33 == 0) + (feat45 == 0)

ppit   =      (feat9 ==1) + (feat15==1) + (feat21 == 1) +
              (feat27 == 1) + (feat33 == 1) + (feat45 == 1)

pchan =      (feat9 ==2) + (feat15==2) + (feat21 == 2) +
              (feat27 == 2) + (feat33 == 2) + (feat45 == 2)

ppass =      (feat9 ==3) + (feat15==3) + (feat21 == 3) +
              (feat27 == 3) + (feat33 == 3) + (feat45 == 3)

pridg =      (feat9 ==4) + (feat15==4) + (feat21 == 4) +
              (feat27 == 4) + (feat33 == 4) + (feat45 == 4)

ppeak =      (feat9 ==5) + (feat15==5) + (feat21 == 5) +
              (feat27 == 5) + (feat33 == 5) + (feat45 == 5)

entrop = 1000* ((pplne/6.0)*log(.001 + pplne/6.0) +
                  (ppit/6.0)*log(.001 + ppit/6.0) +
                  (pchan/6.0)*log(.001 + pchan/6.0) +
                  (ppass/6.0)*log(.001 + ppass/6.0) +
                  (pridg/6.0)*log(.001 + pridg/6.0) +
                  (ppeak/6.0)*log(.001 + ppeak/6.0)) /
                  log(1.0/6.0)

mode =      (max(pplne,ppit,pchan,ppass,pridg,ppeak)==pplne)*0 +
              (max(pplne,ppit,pchan,ppass,pridg,ppeak)==ppit)*1 +
              (max(pplne,ppit,pchan,ppass,pridg,ppeak)==pchan)*2 +
              (max(pplne,ppit,pchan,ppass,pridg,ppeak)==ppass)*3 +
              (max(pplne,ppit,pchan,ppass,pridg,ppeak)==pridg)*4 +
              (max(pplne,ppit,pchan,ppass,pridg,ppeak)==ppeak)*5

EOF

```

5.4 Hydrological Modelling

One of the most direct relationships between geomorphological form and process is that between fluvial and hydrological process and resultant features. This is one of the most widely examined relationships that may be derived from a DEM (see section 2.3). There are several reasons for this pertinent to the objectives of this study. Firstly, although fluvial process results in geomorphological form, the process may be inferred from the nature of that form at the scale of the DEM. This is a relatively rare two way relationship (compare, for example, with other process such as frost heave, longshore drift, weathering etc.). It suggests that the use of GIS-based analysis of DEMs can progress beyond the characterisation of form to an assessment of surface process. Consequently fluvial and hydrological modelling have many immediate applications in the GIS arena. Secondly, fluvially eroded channels are comparatively unambiguously defined geomorphological features that can be represented using a DEM. There is of course, a scale dependency in the effectiveness of this channel modelling. Thirdly, and most importantly in the context of this study, hydrological processes allow us to define important spatial properties of a surface. The drainage basin represents a fundamental geomorphological areal unit, providing both an hierarchical and exhaustive spatial sub-division. Its clear scale dependency is appropriate to the style of analysis adopted in this study, and so will be considered in a little more detail here.

This section will not consider the extraction of drainage networks explicitly. This has been investigated by many authors elsewhere (see section 2.3). It has already been suggested that many of the problems associated with drainage network identification are due to a failure to consider an appropriate range of scales in classification. Some of these problems could be overcome by adopting the multi-scale feature classification described in the previous section. The connected macro-scale valley networks identified with larger kernels can be used to force hydrological connectivity at the raster cell scale. For more details of this style of approach (albeit in a rather more primitive form) see Wood (1990*b*).

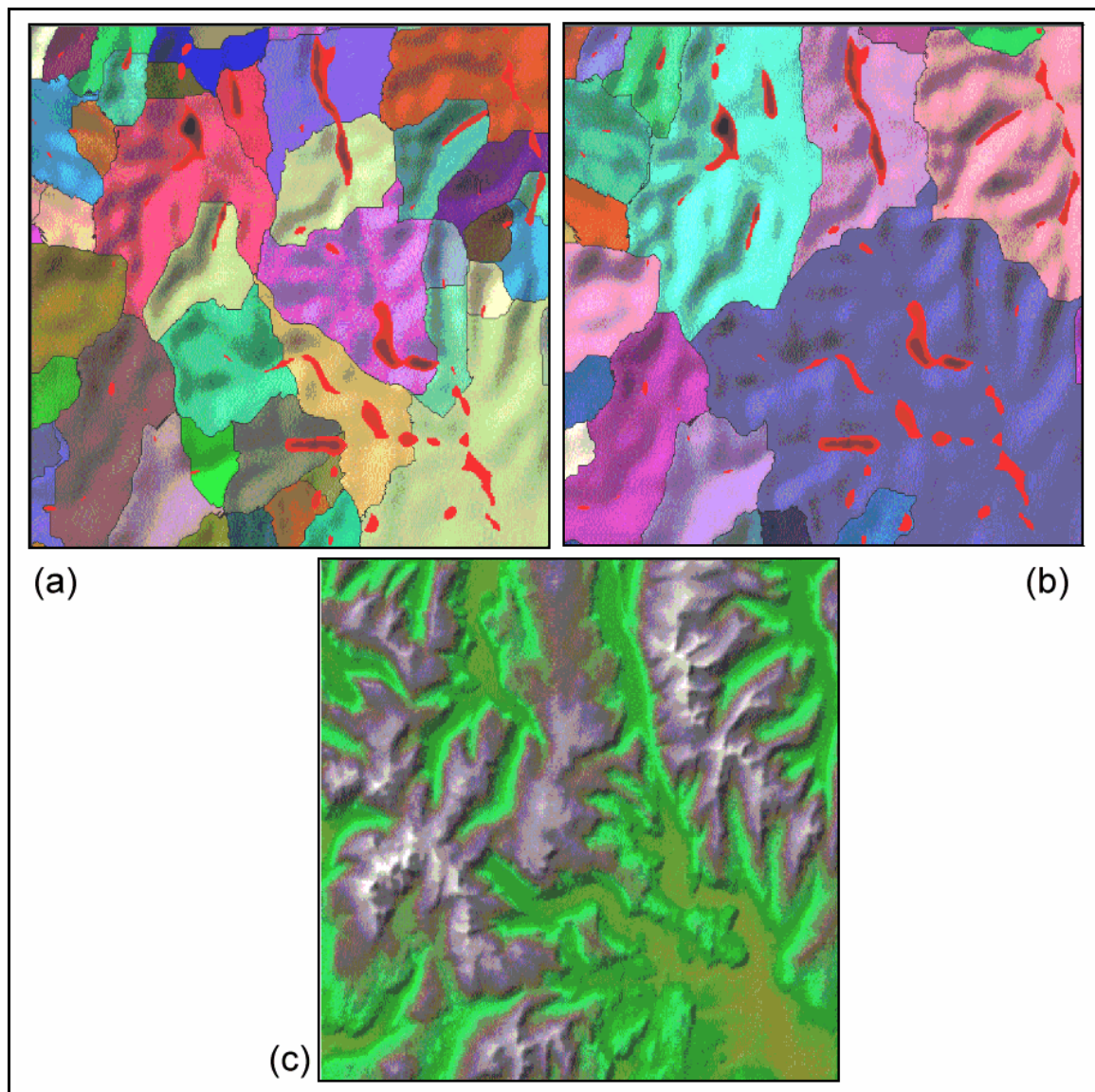
5.4.1 Drainage basin identification

The identification of the drainage basin is an important process in both characterising a surface and in defining spatial units that are appropriately related to geomorphological process. The method for basin identification adopted here also identifies two allied and important surface characteristics. Firstly, basin delineation implies the identification of drainage divides - a linear network whose topology and geometry provide useful summaries of a surface's form. Secondly, a modelled *flow magnitude* surface is produced. Each location on this surface has a value associated with the proportion of surface flow that might be expected to pass over it. This has long been used to identify drainage networks (eg Mark, 1983a). The topology of this surface could be characterised in much the same way as blue-line drainage networks (Shreve, 1966).

Most basin identification algorithms involve a 'basin climbing' approach where a basin outflow point is identified and the basin is recursively 'climbed' until all points flowing from the drainage divide have been covered (eg. Marks *et al*, 1983). This is broadly the approach adopted here (see *r.basin* in the Appendix) . There are, however, a number of problems associated with identifying drainage basins in this way. If a single outflow cell is missed at the base of a steep sided valley, diagonal or orthogonal basin edges can be produced running up the sides of the valley walls. If hydrological consistency is required, pits in the surface halt recursive algorithms that only travel 'upstream' from an outlet (eg Band, 1989). The result is either a basin identification routine that does not work, or the production of internal basins with no apparent outflow. Yet the occurrence of measured pits is relatively common in mountainous terrain where the valley neck is narrow (eg cirque formation). The valley neck itself may not be picked up at the (planimetric) scale of the DEM, or the terrain at the neck may be sufficiently flat to allow elevation uncertainty to dominate.

A number of possible solutions may be applied to this 'problem'. Pits can be filtered out as a preprocessing option. This may however, (arbitrarily) change elevation values unnecessarily. Alternatively, internal basins may be merged as a post-processing operation. This may be achieved by either 'excavating' cells that connect the base of a pit to its adjacent downstream basin, or by flooding pits until outflow is redirected. The latter is adopted here (see *r.basin* in the Appendix). Figure 5.8 shows the effect of recursive pit removal on basin derivation for a

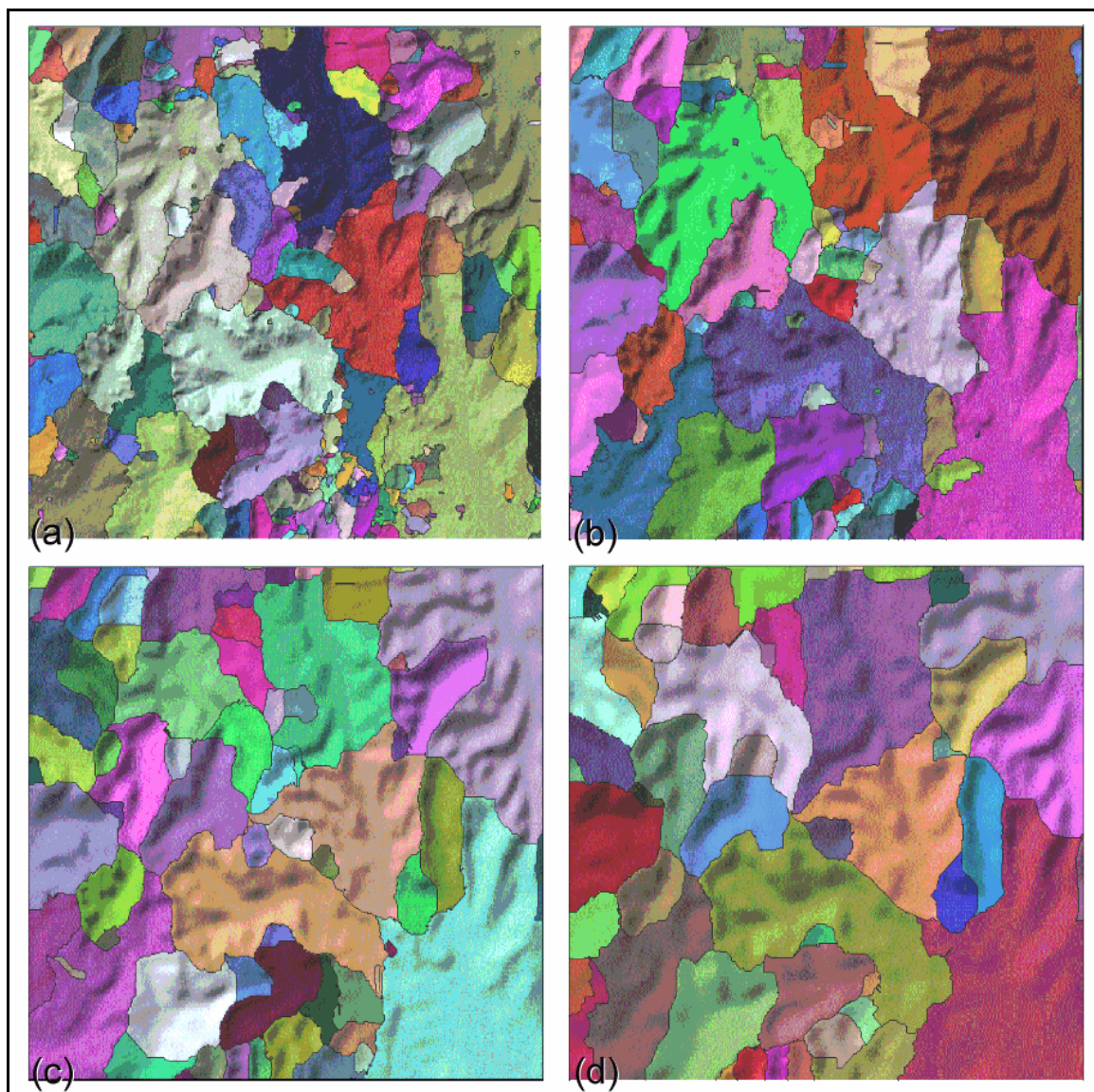
30x30km region of the Lake District. Superimposed on (a) and (b) is the distribution of flooded pits (in shades of red). In all cases, internal basins (a) contain at least one of these pits. The basins in Figure 5.8(b) correspond to the major valley systems of this part of the Lake District (clockwise from the top, *cyan*, Borrowdale; *mauve*, Thirlmere valley; *pink*, Ullswater valley;



blue, Windermere/Coniston valleys; *purple*, Dunnerdale; *plum* Eskdale; *pink*, Wasdale).

For geomorphological characterisation (as opposed to hydrological analysis) it is arguable whether the identification of internal drainage basins is in fact a problem. Valley systems with narrow necks *should* be represented as pits at some scale. It is only a problem for hydrological

modelling that the mechanism for water removal is expressed at a different scale. The relationship between basin delineation (not hydrologically enforced) and scale is shown in Figure 5.9. Quadratic approximation is used to smooth the DEM with kernel sizes up to 950m. The basin finding routine was then applied to the smoothed surfaces. As expected the number of basins decreases with generalisation, although not spatially consistent.



Chapter Six - Results.

This chapter contains an assessment of the DEM characterisation tools that have been developed in the previous chapters. This takes three forms; a theoretical evaluation of a technique's validity; a calibration of the visualisation tools; and an investigation into a technique's utility through application.

A theoretical evaluation has, in part, already been discussed in the previous three chapters. Since many of the techniques used involve the quadratic approximation of local surface patches, the implications of this form of modelling will be assessed in greater detail. The more abstracted measurements and their visualisation (for example, the lag diagrams discussed in section 4.5) require some form of calibration where the geomorphometric analysis yields measurements that are not intuitively obvious. This is most effectively carried out by applying such measures to surfaces with simple and known properties. These can then be applied to surfaces whose properties are not known. Finally the utility of the techniques and methodology proposed is illustrated with the analysis of 'real' topographic surfaces.

6.1 Control Surfaces.

The evaluation of characterisation tools involves using some control surfaces whose properties are known or can be systematically altered. This section outlines their derivation and utility.

6.1.1 Uncorrelated Gaussian Surfaces.

If one of the objectives of surface characterisation is to identify spatial structure, it is useful to make comparison with surfaces that have no spatial structure at all. For the purpose of this study, a GRASS module, *r.gauss.surf* was written (see Appendix) that generates an uncorrelated random surface with a Gaussian (normal) distribution. The resolution, size, mean and standard deviation can all be controlled from the program.

The *Box-Muller* method is used for generating the random deviates with Gaussian distribution

(see Press *et al*, 1992, pp.288-290). This involves transforming two uniform random deviates between 0 and 1 (x_1 and x_2) as follows,

$$y_1 = \sqrt{-2 \ln x_1} \cdot \cos(2\pi x_2)$$

$$y_2 = \sqrt{-2 \ln x_1} \cdot \sin(2\pi x_2)$$

$$G(y_1, y_2) = -\left[\frac{1}{\sqrt{2\pi}} e^{-y_1^2/2} \right] \left[\frac{1}{\sqrt{2\pi}} e^{-y_2^2/2} \right]$$

6.1.2 Object Surfaces.

Alternatively, a control may be used that has a high degree of spatial structure. Such surfaces are particularly useful for calibrating lag diagrams (for example, see the discussion on measures of spatial autocorrelation, section 4.5.1).

To create simple geometric objects within GRASS, a module *r.xy* (see Appendix) was written that creates two raster surfaces based on the coordinates of each cell location. An origin is set at the bottom left corner, with unit coordinate displacement,

$$\begin{aligned} f(x, y) &= x \\ f(x, y) &= n\text{rows} - y \end{aligned}$$

These surfaces may be manipulated using map algebra (Tomlin, 1989; Shapiro and Westervelt, 1992), to create simple geometrical surface objects. For example to create a cylinder of height 20 units and of radius 50 units centred over a 201 x 201 cell raster, the following map algebra expression was issued using the GRASS module *r.mapcalc*,

```
circle = if ((x - 101)*(x-101) + (y-101)*(y-101) > 2500, 20, 0)
where x and y are raster layers created using r.xy.
```

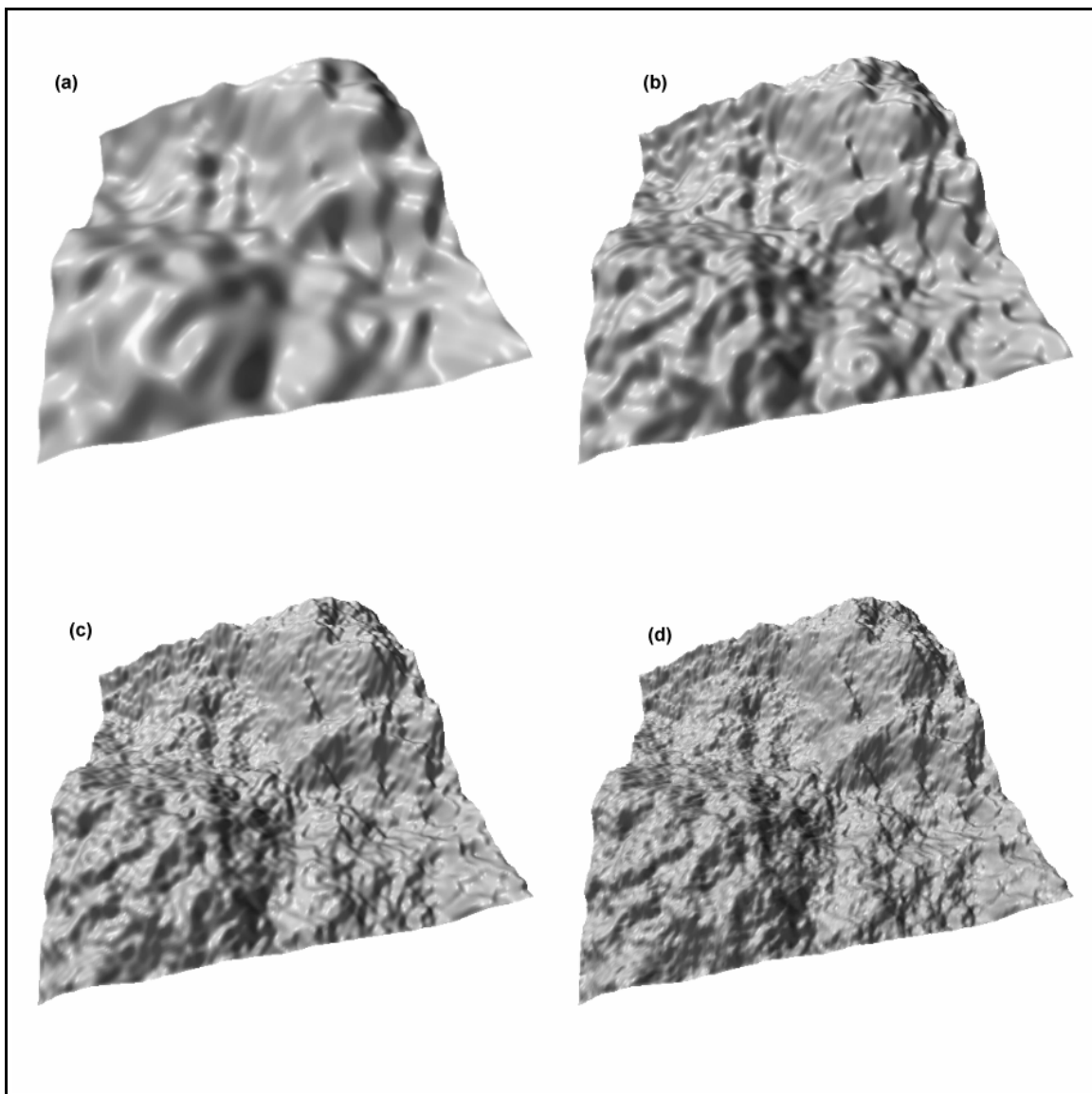
To create a 20 x 20 x 20 unit cube in the top left corner of a 201 x 201 cell raster,

```
cube= if ( (x < 20) && (y>180), 20, 0)
```

6.1.3 Fractal Surfaces

The third form of control surface used in evaluation allows a degree of spatial structure to be controlled. It was originally anticipated that this could be achieved by creating polynomial surfaces of a user-defined order. However, since much of the surface modelling involves quadratic fitting, there is a danger of producing circular evidence. That is, there may be a tendency for quadratic models to fit other polynomial surfaces more effectively than, for example, trigonometric or 'real' surfaces.

Fractal surface generation was adopted as a more realistic but controllable model of topographic variation. By changing the fractal dimension of the surface, the degree of spatial structure can be varied. There are numerous methods of generating fractal surfaces (see section 2.5), but the one adopted here uses the spectral synthesis approach described by Saupe (1988), pp.105-109. This technique involves selecting scaled (Gaussian) random Fourier coefficients and performing the inverse Fourier transform. It has the advantage over the more common midpoint displacement methods which produce characteristic artifacts at distances 2^n units away from a local origin (Voss, 1988). More importantly for this work, this technique has been modified so that multiple surfaces may be realised with only selected Fourier coefficients (see *r.frac.surf* in the Appendix). The result is that the scale of fractal behaviour may be controlled as well as the fractal dimension itself. Figure 6.1 shows a fractal surface of dimension D=2.10 rendered with (a) 1/8th, (b) 1/4, (c) 1/2, and (d) all of the Fourier coefficients transformed.



6.2 Terrain Models

The DEMs representing real terrain were all selected from the Ordnance Survey 1:50k coverage of the UK. Three areas for study were selected that show contrasting topographic variation. It should be remembered that the objective of this study is not to provide a comprehensive characterisation of the UK landscape, but to demonstrate the utility of the characterisation tools themselves.

6.2.1 Lake District

The following Ordnance Survey DEM tiles were used (with National Grid coordinates indicating extent of the coverage),

(360000, 540000)

NY02	NY22	NY42
NY00	NY20	NY40
SD08	SD28	SD48

(300000, 480000)

Each tile consists of 401 x 401 cells of size 50m x 50m, giving a 3600km² coverage of the major part of the Lake District. Various 'sub-windows' were selected for the evaluation below (and previous chapters).

The area represented is a mountainous previously glaciated environment ranging in altitude from sea level to 977m (England's highest mountain). The central upland region (NY20) is dominated by Borrowdale Volcanics, with Skiddaw Slates to the north (NY22) and Silurian shales and sandstones to the south (SD28).

6.2.2 Dartmoor

The following Ordnance Survey tiles covering central Dartmoor were selected,

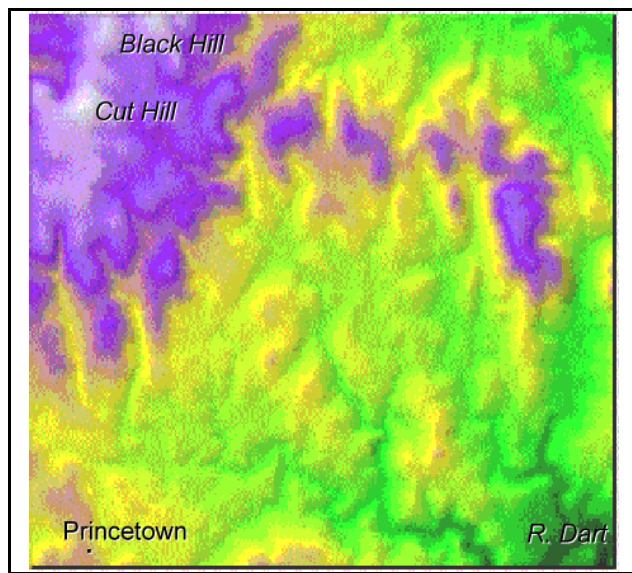
(280000, 100000)

SX48	SX68
SX46	SX66

(240000, 060000)

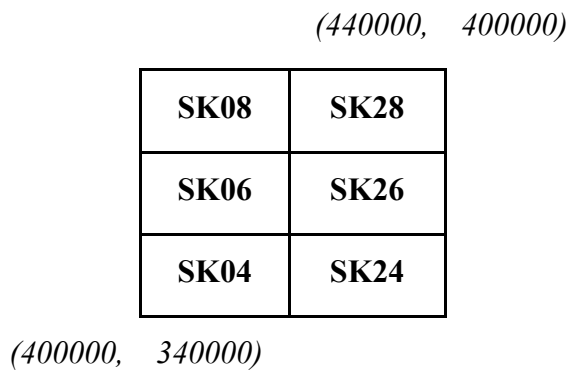
The area is entirely within the surface outcrop of the Dartmoor granitic intrusion giving rise to a characteristic upland 'moor and tor' topography. The extent of the selected DEM is shown in

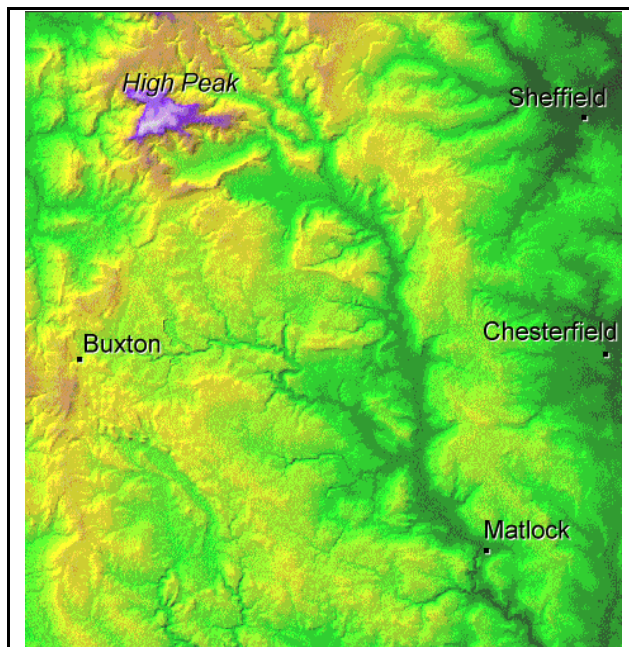
Figure 6.2 (15 x 14 km).



7.2.3 Peak District

The third area selected for study covers a wider 40 x 41km area around the south of the Peak District (40 x 41 km). The Derwent valley runs north-south across the map from the moorland in the High Peak area to the south of the region near Matlock (Figure 6.3). The geology is dominated by Carboniferous Limestone to the west of the Derwent and Millstone Grit to the east and north.





6.3 Assessment of Quadratic Approximation Tools

6.3.1 Non-spatial analysis of residuals.

Even at the 3×3 kernel size, a quadratic function cannot precisely model the 9 values used in its construction. The question arises therefore, does the approximation lose vital surface information, or worse, does it introduce systematic artifacts into the surface model?

To test this question, the pattern of residuals between the quadratic parameter f (elevation at centre of the kernel) and the measured elevation from the DEM was examined. Three surfaces were used for analysis, each with a different degree of spatial structure. Two fractal surfaces of 200×200 cells were created, one with a low fractal dimension ($D=2.01$), the other with a high fractal dimension ($D=2.9$). A third uncorrelated Gaussian surface was created for comparison. Summary statistics for all three layers are shown in Table 6. 1.

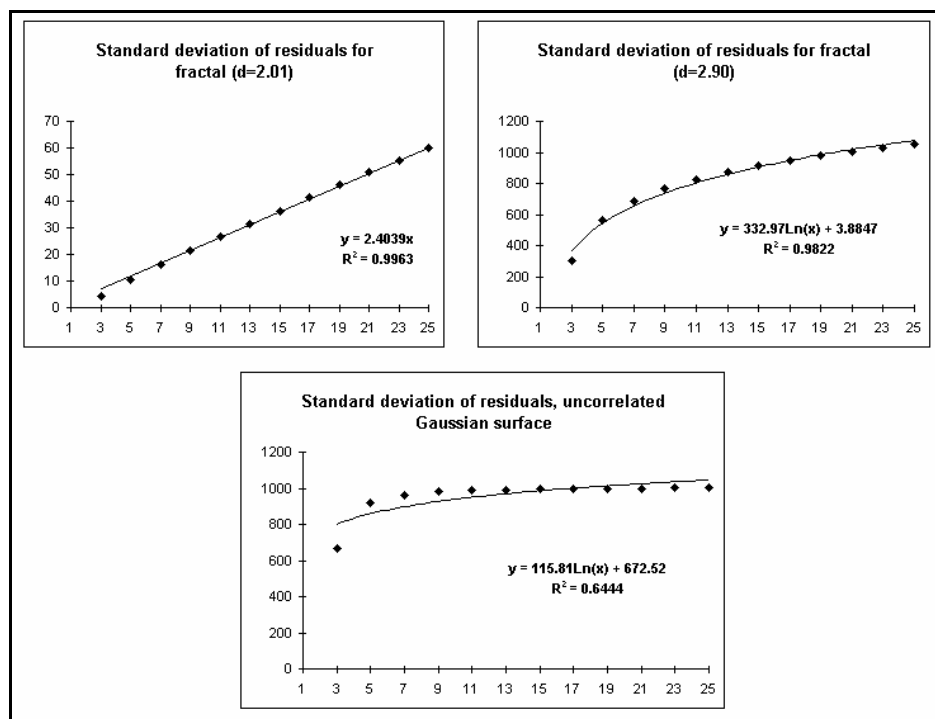
	number of cells	mean	std. dev.
fractal (d=2.01)	40000	-47.32	859.44
fractal (d=2.90)	40000	-152.59	1899.20
Gaussian	40000	1.47	1002.13

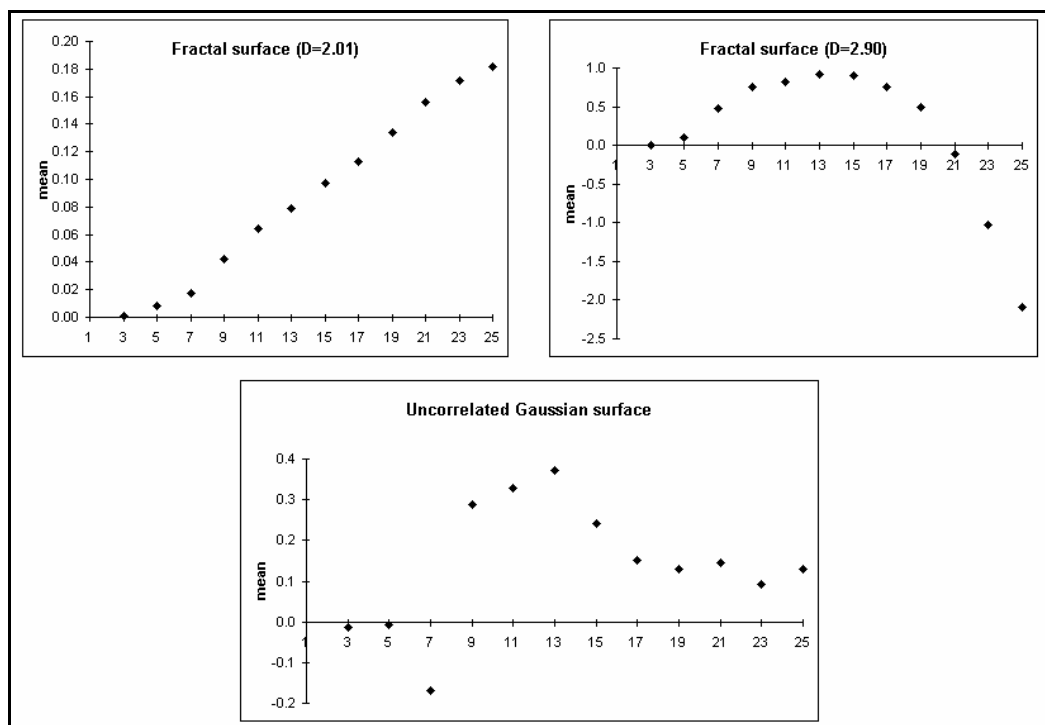
Table 6.1 - Summary statistics of quadratic control surfaces.

Table 6.2 shows the mean and standard deviation of the residuals for various kernel sizes. As expected, the standard deviation increases with larger kernels (where the quadratic function becomes increasingly overspecified). The nature of the relationship between residuals and kernel size is shown in Figures 6.2 and 6.3.

Kernel size	fractal d=2.01		fractal, d=2.90		Gaussian	
	mean	stdev	mean	stdev	mean	stdev
3 x 3	0.001	4.11	0.007	302.45	-0.013	667.31
5 x 5	0.008	10.51	0.104	563.99	-0.006	922.67
7 x 7	0.017	16.02	0.478	688.82	-0.170	964.23
9 x 9	0.042	21.35	0.760	768.50	0.287	981.03
11 x 11	0.064	26.50	0.815	825.24	0.329	987.91
13 x 13	0.079	31.49	0.914	870.59	0.371	992.57
15 x 15	0.097	36.42	0.904	910.88	0.242	995.75
17 x 17	0.113	41.29	0.756	945.56	0.150	997.72
19 x 19	0.134	46.09	0.499	975.92	0.129	999.30
21 x 21	0.156	50.79	-0.118	1003.27	0.145	999.77
23 x 23	0.172	55.37	-1.026	1028.13	0.092	1000.50
25 x 25	0.182	59.80	-2.097	1051.89	0.129	1000.92

Table 6.2 - Summary statistics for quadratic approximation residuals for various kernel sizes.





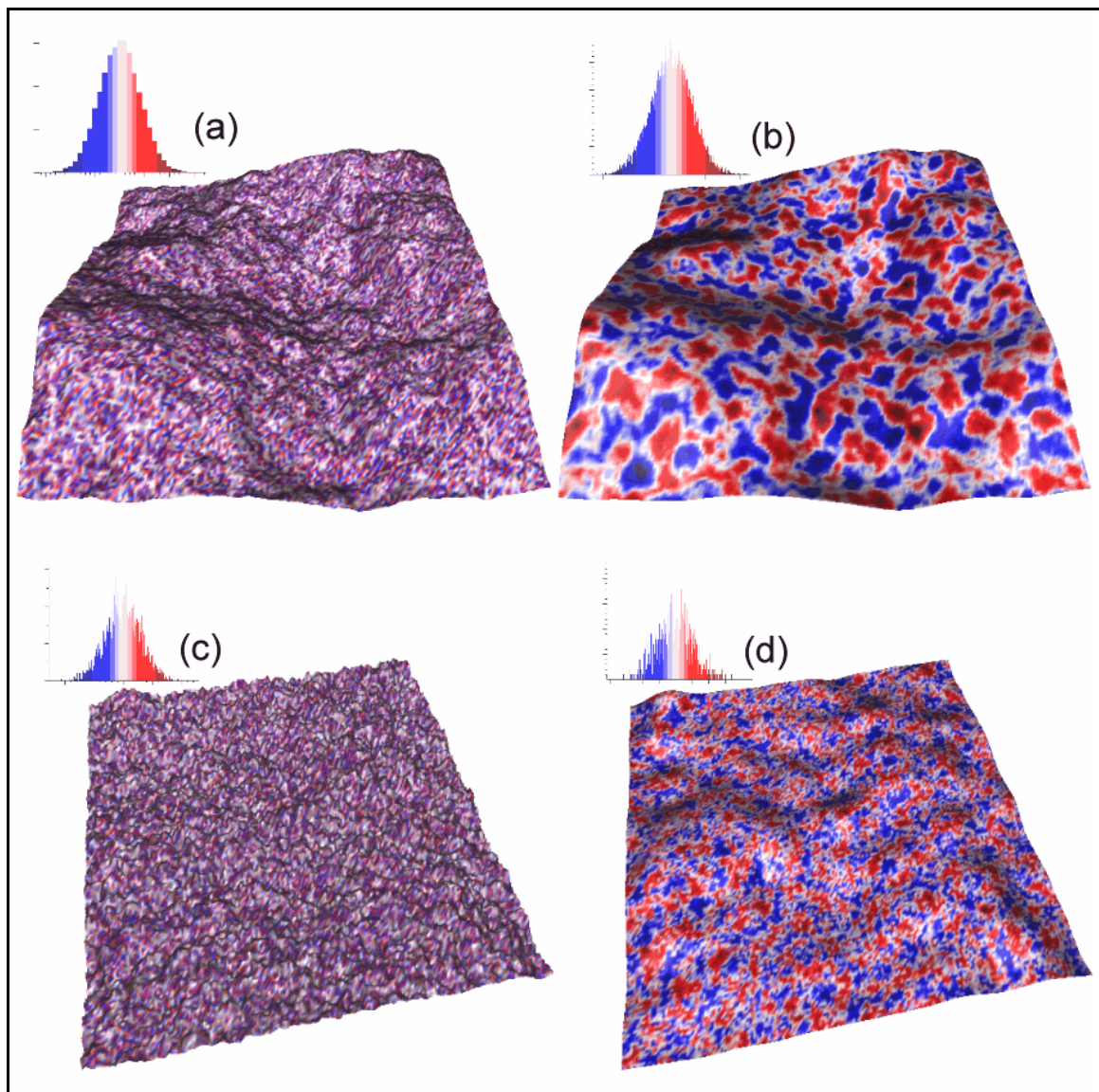
For the surfaces with the greatest spatial autocorrelation (fractal $D=2.01$), there appears a well defined ($R^2=0.996$) linear relationship between kernel size and the magnitude of the residual between quadratic model and original elevation. This suggests that the degree of approximation

of 'smooth' surfaces can be controlled entirely by kernel size. As the surface becomes 'rougher' there appears a well defined ($R^2=0.902$) log-linear relationship between residuals and kernel size. The transition from linear to log-linear relationship suggests that for rougher surfaces there is a degree of 'diminishing returns' with increasing spatial approximation. That is, most approximation occurs at smaller spatial scales with little further generalisation introduced by larger kernels. This relationship is exemplified by the case of the uncorrelated surface where there is little control over residual magnitude beyond a kernel size of 7 x 7 cells.

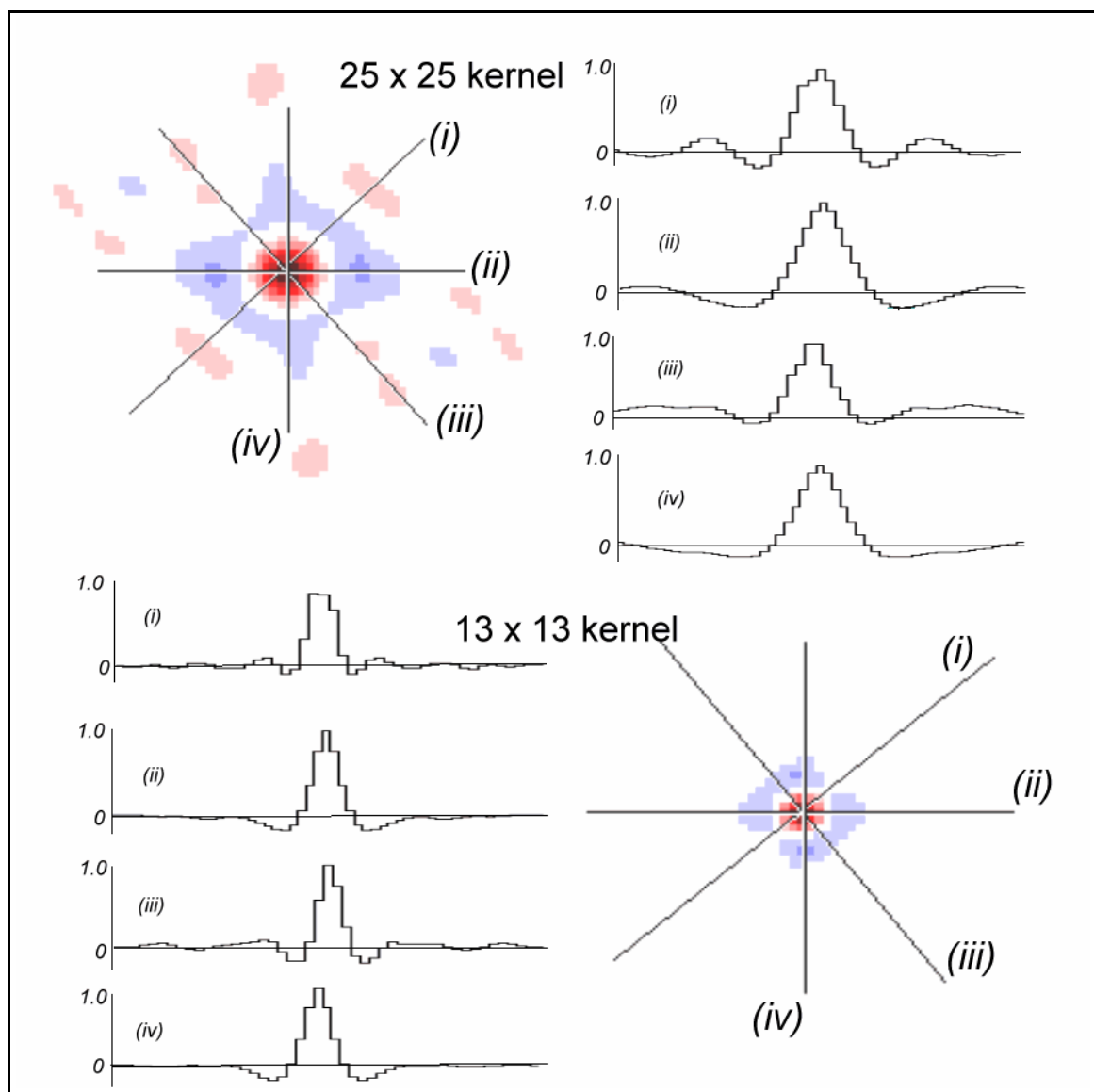
The relationship between kernel size and residual mean (Figure 6.3) should indicate any systematic over- or under- estimates of elevation. The magnitude of maximum residual mean is less than 0.5% of the residual standard deviation, and so in practice, will have very little systematic effect on elevation estimates. It is worth noting however, that the degree of over- or under-estimation of elevation appears to be dependent the topographic form as well as kernel size. For example, a DEM representing a single valley system will tend to produce consistently higher overestimates of elevation as kernel size is increased. Likewise, a tendency to regress towards a mean elevation will produce increasingly large underestimates of elevation for a DEM representing a single peak.

6.3.2 Spatial analysis of residuals

As with the discussion of DEM uncertainty (see Chapter 3), global measures of elevation variation are not sufficient to understand the pattern of residuals, since they are likely to vary over space. Figure 6.4 shows selected 'residual maps' for the quadratic approximation of the two fractal surfaces at different scales.



All four images in Figure 6.4 show some form of spatial clustering of residuals, that not unexpectedly corresponds with a change in kernel size. To describe the spatial pattern in more systematically, Moran's I lag diagrams (see section 4.5) were visualised. Figure 6.5 shows two selected examples corresponding to residuals produced by 25x25 and 13x13 cell kernels. Red indicates positive autocorrelation, blue negative. The magnitude of the statistic is additionally shown with selected profiles.

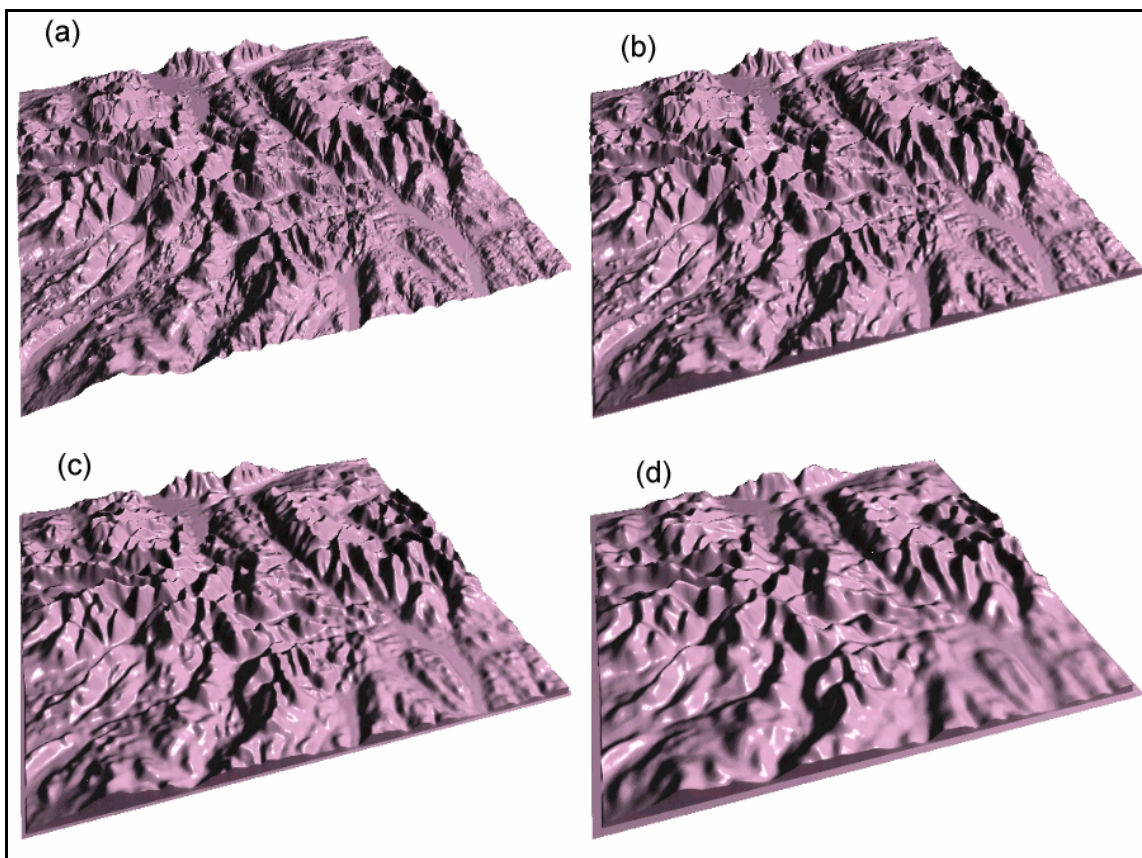


The clustering seen in Figure 6.4 is described by the high spatial autocorrelation at low lags. Spatial autocorrelation is reduced as lag increases, reaching a minimum value before becoming approximately uncorrelated. In both cases, the innermost uncorrelated (white) band corresponds to approximately half the kernel size, while the maximum negative value is at approximately 2/3 the kernel width. There is also a degree of anisotropy shown by the lag diagrams as 'diamond' rather than circular bands of equal autocorrelation. This is due to the square shape of the kernel that was used without any form of distance weighting. These findings suggest that filters that do not have any kind of distance weighting may well have to be treated with caution, especially when processing surfaces with low spatial autocorrelation at the scale of the filter.

6.3.3 Quadratic approximation as a surface generalisation tool

The effectiveness of quadratic approximation as a generalisation process was examined by comparing the smoothing effect of mean convolution filtering (the most common form of surface smoothing) with that of quadratic approximation.

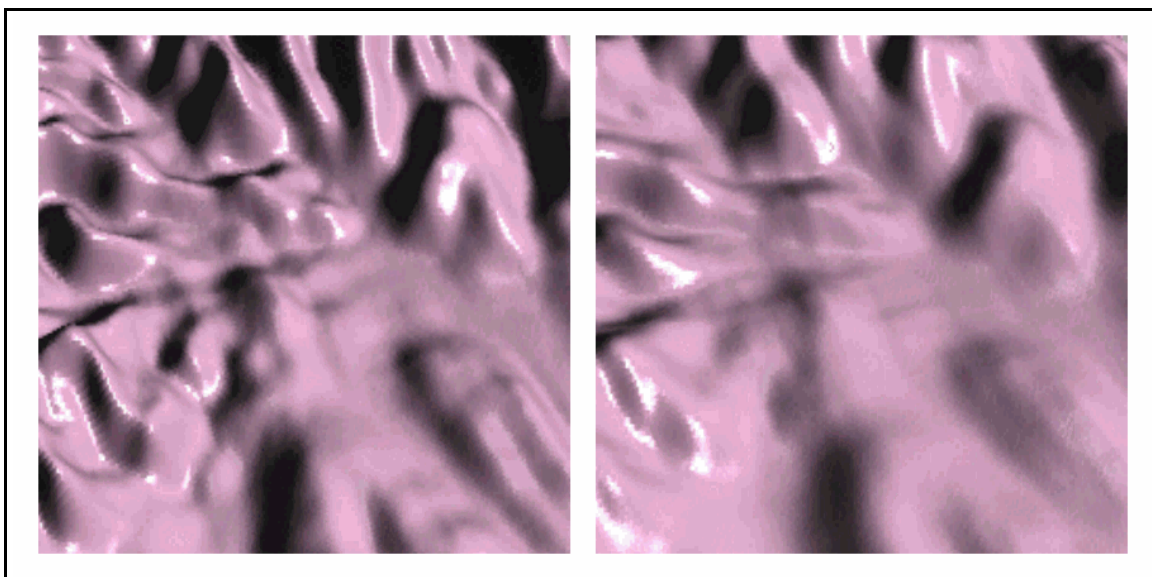
Figure 6.6 shows the visual effect of quadratic approximation as a generalisation process, applied to the central Lake District (35km x 35km). Kernel sizes range from 7x7 (350m) to 25x25 cells (1.25km).



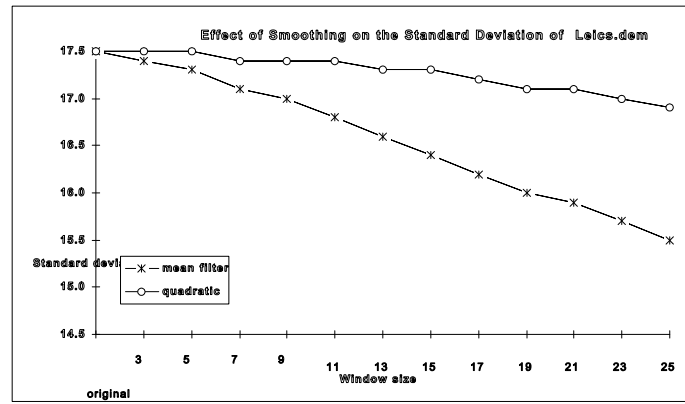
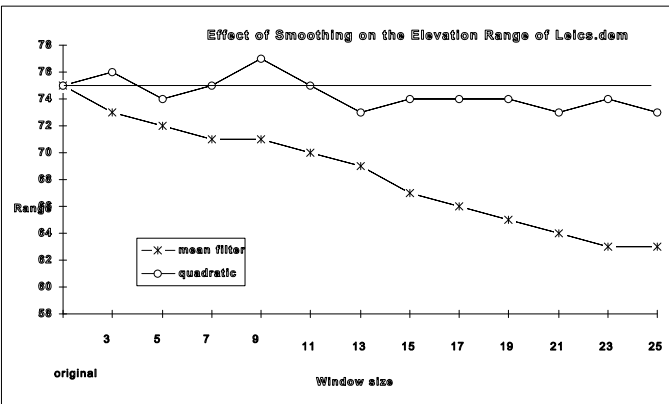
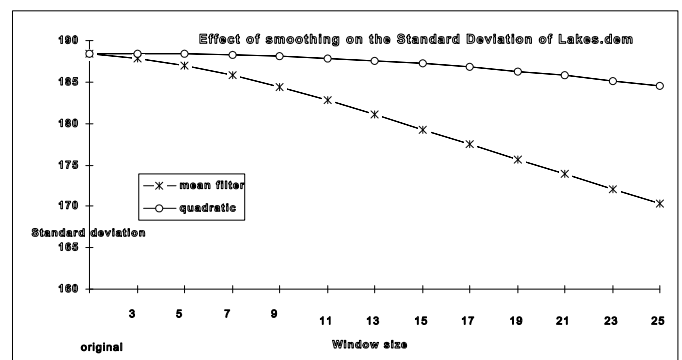
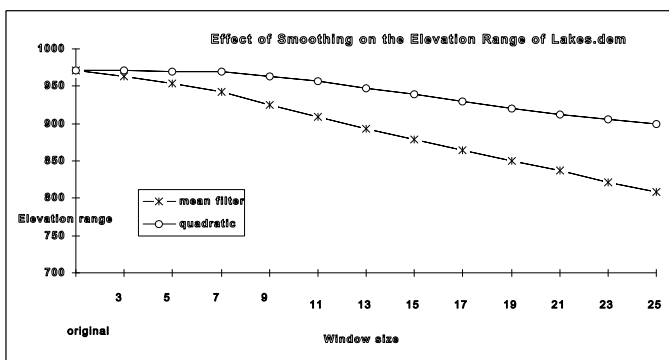
The effect of non-distance weighted quadratic smoothing on the frequency distribution properties of three surfaces was considered. The range and standard deviation of (i) an uncorrelated Gaussian surface, (ii) the Lake District DEM pictured in Figure 6.6; and (iii) the Leicestershire

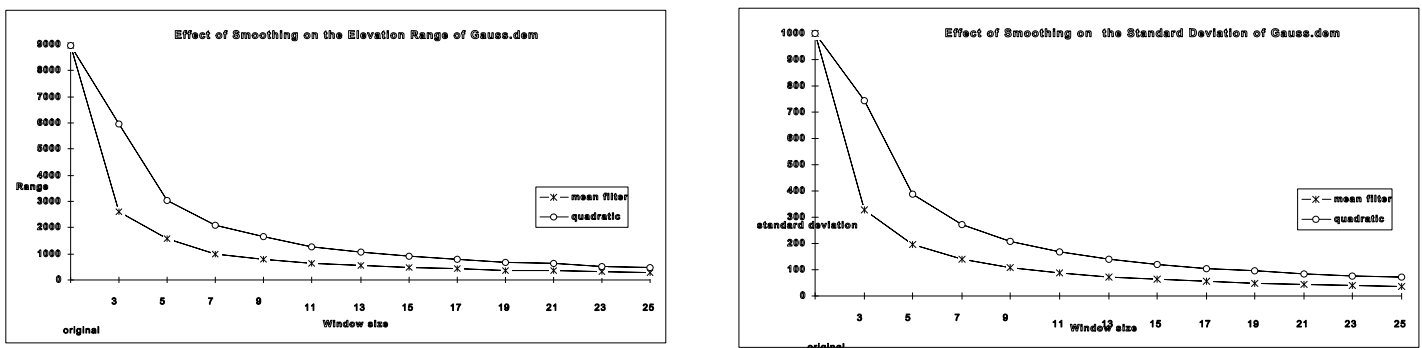
DEM were examined after filtering at all scales from 3x3 to 25x25 cells. Comparison was made with a non-distance weighted mean filter (using the GRASS program *r.mfilter*) at the same range of scales. Figure 6.8a-f show the relationship between elevation dispersion and kernel size. Note also, the non-linear smoothing effect of the Gaussian surface that was also observed in section 6.3.1.

As would be expected, the larger the filter, the greater the reduction in range and variance of elevation values. However quadratic smoothing retains the original global dispersion characteristics far more effectively than mean filtering. This is reinforced by visualising the smoothed surfaces. Figure 6.7 shows the south east corner of the Lake District DEM (Windermere/Ambleside) smoothed using both the 25x25 quadratic and mean filters. Quadratic approximation appears to preserve characteristics at the certain scales while smoothing detail at



finer scales. Mean filtering would appear far more scale insensitive in its smoothing effects.



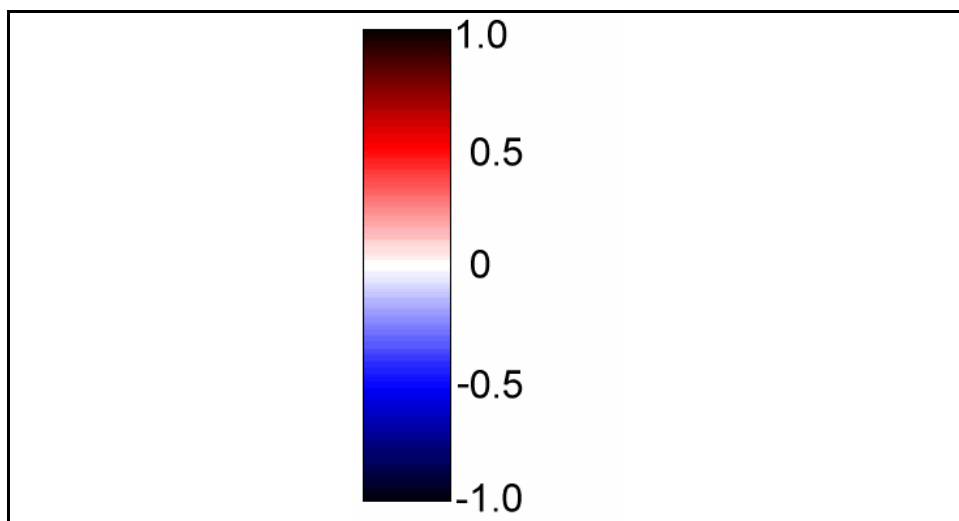


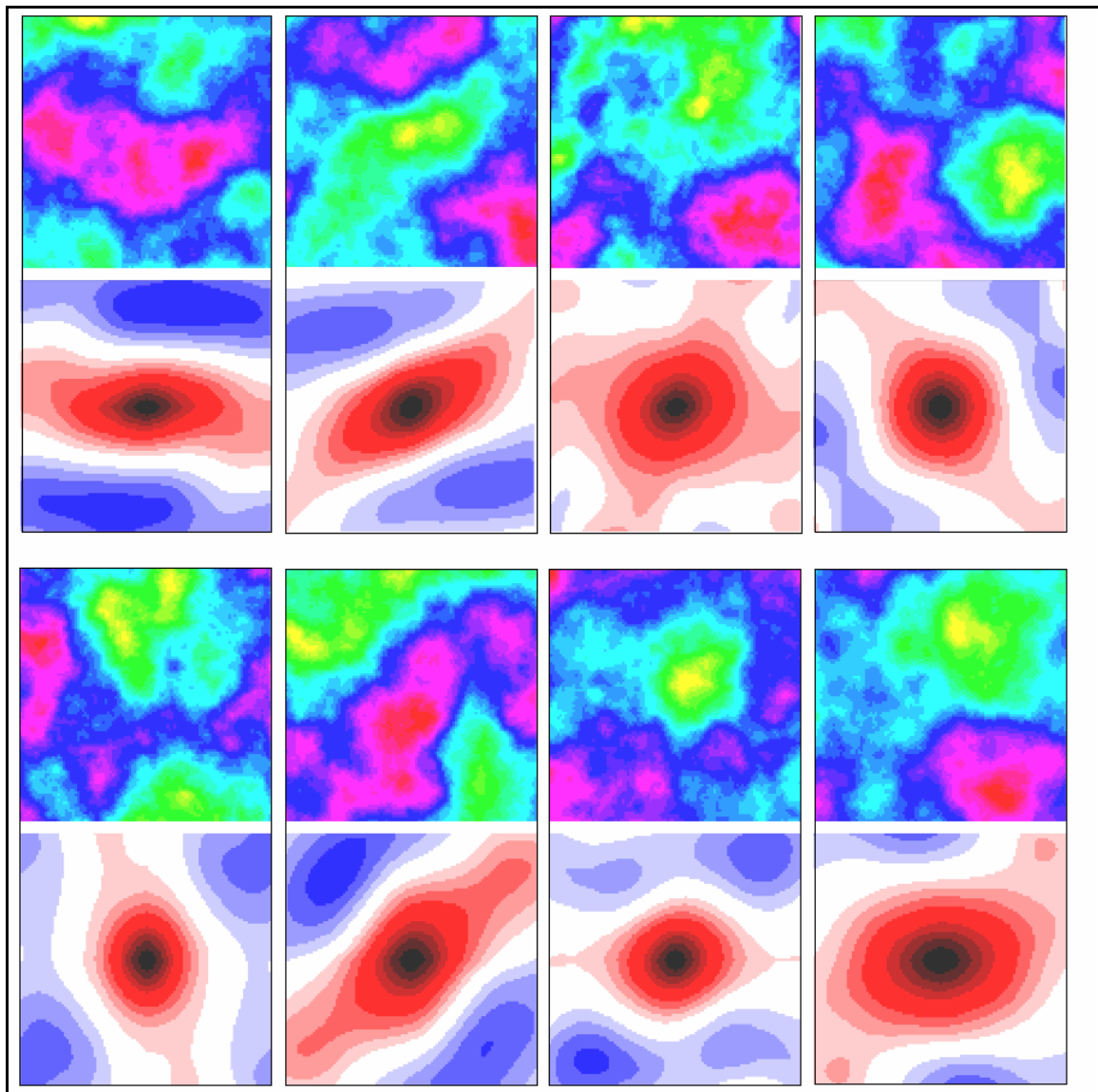
6.4 Calibration of Spatial Dependence Measures.

Section 4.5 described how several tools were developed to visualise and measure the spatial structure of DEMs. This section evaluates their utility by 'calibrating' them with surfaces with known properties.

It was suggested that a lag diagram of Moran's I spatial autocorrelation index could reveal something of the relationship between spatial dependence and scale. To evaluate this, multiple realisations of a fractal surface were generated. Eight surfaces of fractal dimension $D=2.10$ were

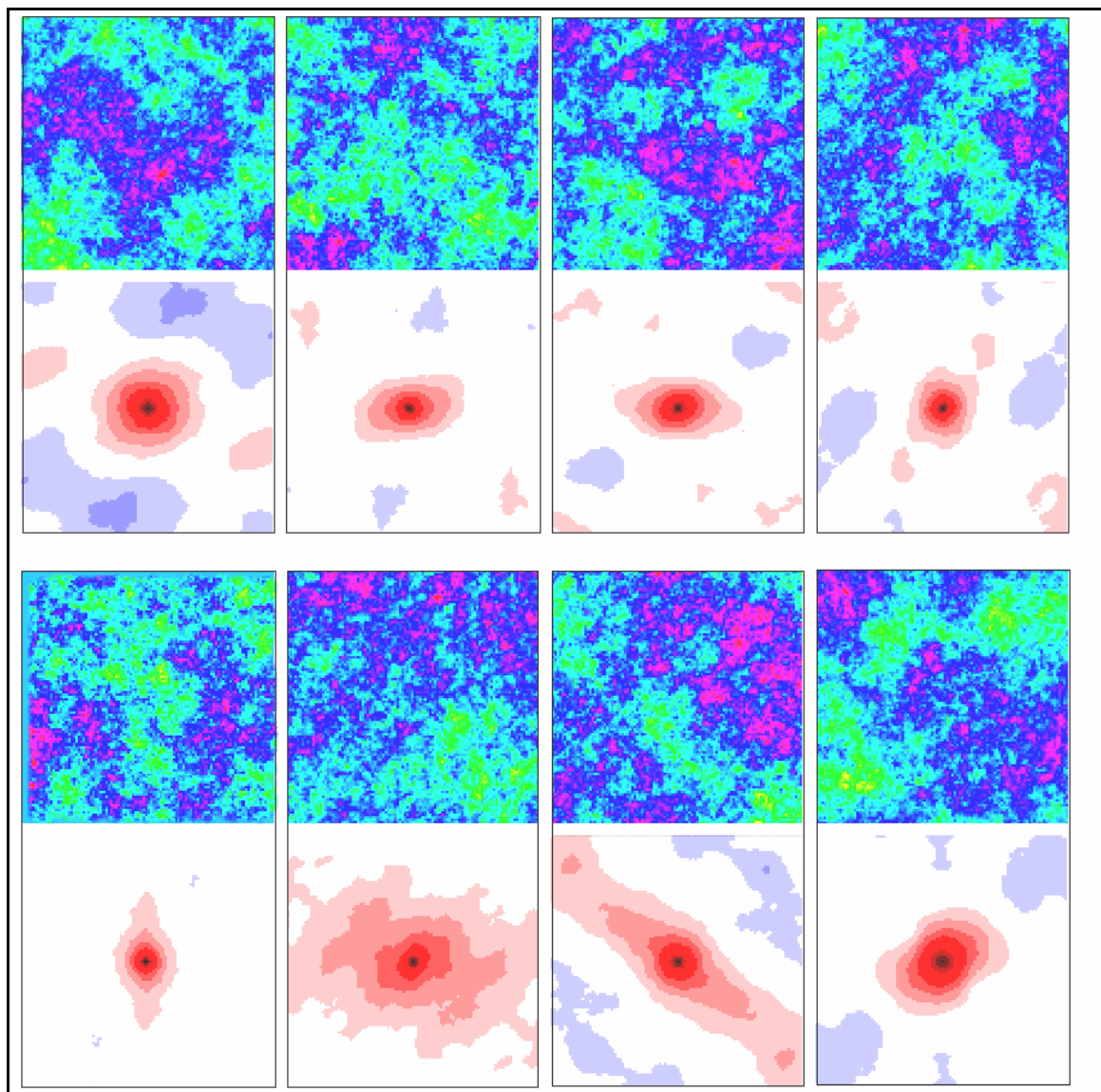
created, and eight of $D=2.90$. A lag diagram of Moran's I was generated for each surface. Figures 6.10 and 6.11 show the results for surfaces with $D=2.10$ and $D=2.90$ respectively. The bi-polar colour scheme used for all Moran diagrams is shown in Figure 6.9.





The notion of a distinction between *texture* and *structure* is a common one in image processing (eg Gonzalez and Woods, 1992) and is useful to consider here. All the surfaces shown in Figure 6.10 have similar (fine scale) textural characteristics (determined by the fractal dimension), but structurally (coarse scale) they vary. That is, due to the random generation of Fourier coefficients, a surface may describe on a low frequency peak, pit, ridge, channel or combination of features. What distinguishes texture from structure is simply the scale at which variation is considered. All the images in Figure 6.10 show similar fine scale variation, in that the central portions of all lag diagrams are similar. Variation tends to occur away from the centre seen as concentric zones of equal spatial autocorrelation. The most obvious feature of these larger lag measures, is the ability to represent anisotropy. The orientation of any coarse scale valley or

ridge systems is picked out by elongated bands of equal spatial autocorrelation. In several cases such bands tend to 'twist' with increasing lag suggesting a change of orientation with scale. It should be noted that such variation would not be detected using the traditional (one-dimensional) variogram. Surfaces without a dominant ridge or valley system tend to produce lag diagrams with a greater proportion of positively autocorrelated measurements.

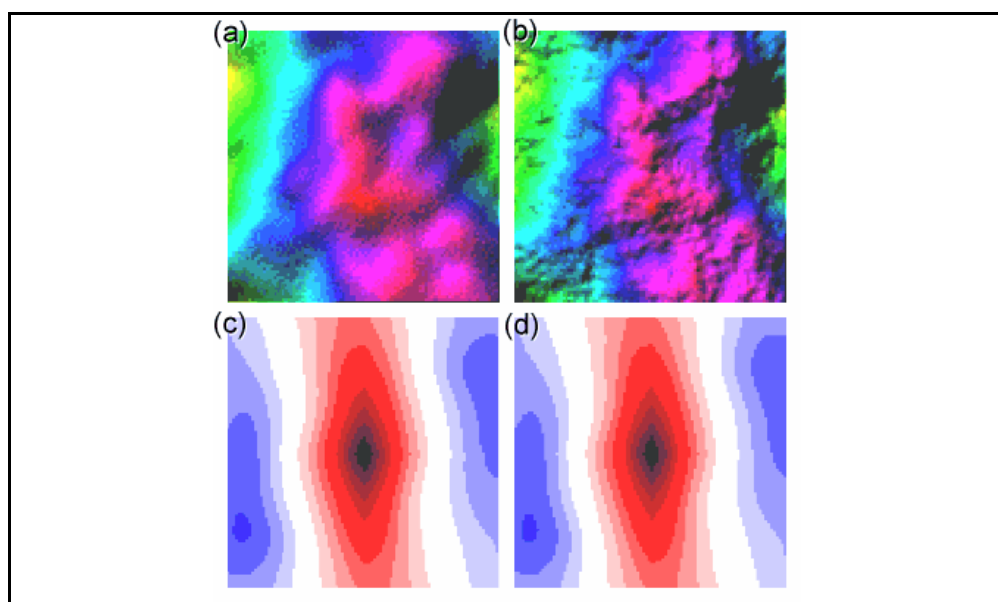


The eight sets of images shown in Figure 6.11 show a marked contrast with the surfaces of lower fractal dimension. Generally, the magnitude of either positive or negative autocorrelation is lower (images appear 'paler'). The characteristic diameter of high spatial autocorrelation is much

smaller for these rougher surfaces. Coarse scale structure and anisotropy is still revealed, albeit less strongly.

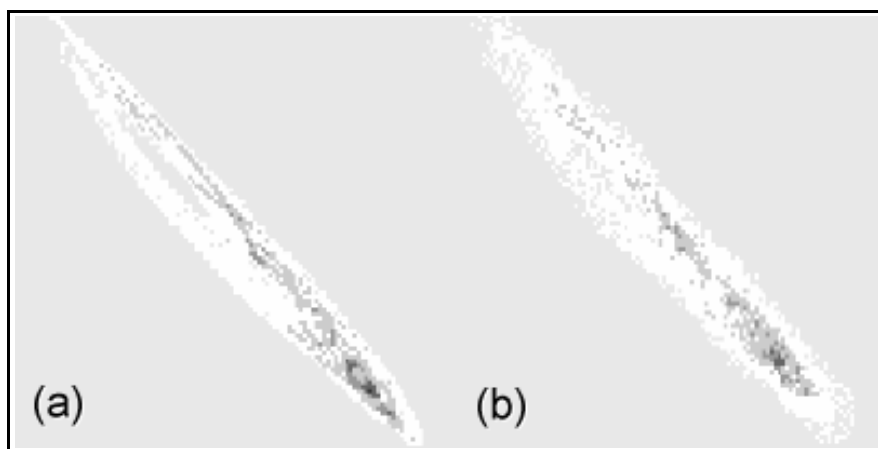
It would appear that Moran's *I* lag diagrams are useful in detecting structural variation and anisotropy, and the relative dominance of textural and structural components of surface form. Although the terms texture and structure are used, these diagrams show the scale based continuum between the two rather than forcing an artificial dichotomy between them. To investigate the distinction between textural and structural variation further, a second set of fractal surfaces was produced. Using a single set of scaled Gaussian Fourier coefficients, selected coefficients were transformed. The effect was to generate a series of similar surfaces but each with increasingly high frequency detail added (see Figure 6.1 for an example).

Figure 6.12 shows two surfaces from the series, one with 1/8th of the Fourier coefficients transformed, the other with all coefficients. Surface texture is emphasised by combining elevation and local relief as a hue-intensity map. The Moran's *I* lag diagrams for both surfaces are shown below.



The two lag diagrams appear very similar, suggesting that they are not suitable visualisations of high frequency textural variation. Indeed, visualising the original surfaces (Figure 6.12a and b) is much more useful. This demonstrates that such lag diagrams are dominated by, and therefore most suitable for examining, structural variation. The change in texture between the two surfaces occurs only in the immediate (dark) central portion of each image.

To examine finer scale textural variation , co-occurrence textural measures were investigated (see also section 4.5.2). The co-occurrence matrices for the two surfaces shown in Figure 6.12 were calculated and textural measures calculated from them. A visualisation of the two matrices is shown in Figure 6.13 and the derived texture measures are recorded in Table 6.3.

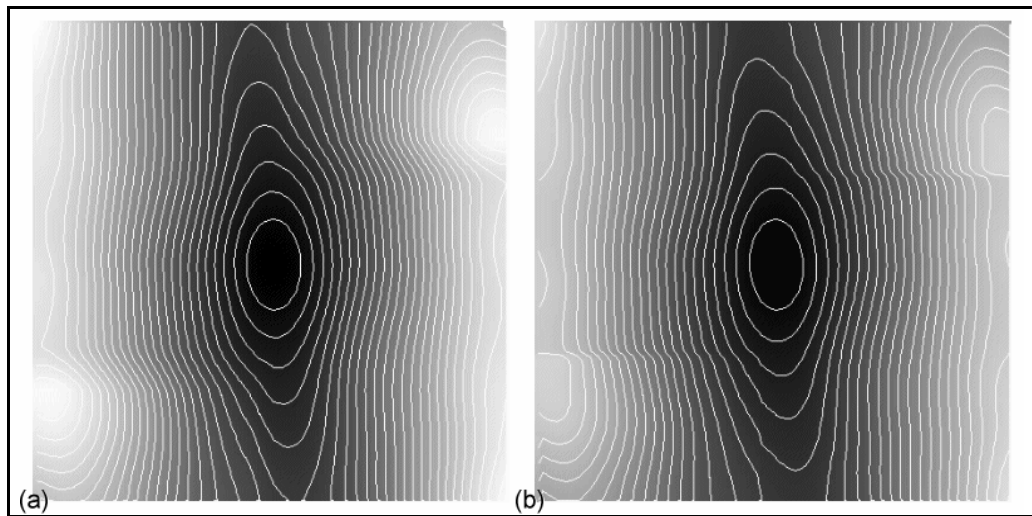


Texture Measure	fractal (1/8th coeff.)	fractal (all coeff.)
<i>Contrast</i>	22.85	26.03
<i>Angular Second Moment</i>	0.0012	0.0010
<i>Entropy</i>	6.99	7.15
<i>Asymmetry</i>	0.00071	0.00042
<i>Inverse Distance Moment</i>	0.064	0.068

Table 6.3 - Selected texture measures for the two fractal surfaces.

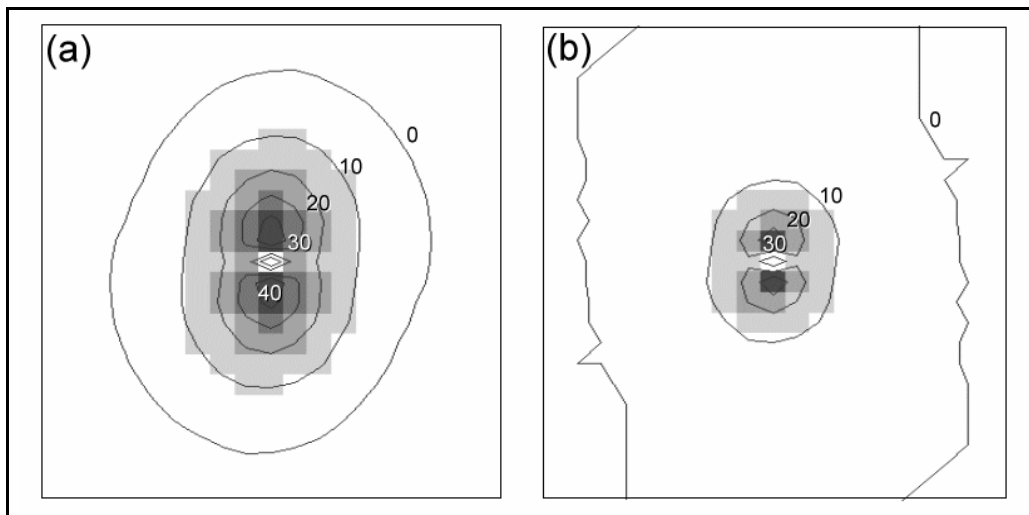
The global textural measures do appear to discriminate between the two surfaces although it is not clear which distinct texture properties each measure. The co-occurrence matrix itself also appears to vary between the surfaces with the rougher surface producing the more disperse matrix. However, it should be considered that both the matrix and the derived indices are measured at a single lag (unit offset in this case). It would be expected therefore, that they should show different patterns at different scales.

To determine any scale dependency in textural characteristics, lag diagrams were calculated for two of the measures - contrast and inverse distance moment. The others were excluded either because they are scaled variations of the same property or because they showed no scale dependency. Figure 6.14 shows the contrast lag diagram for the two surfaces. Darker shading indicates lower contrast. Contours at 500 unit intervals are included to emphasise surface variation.



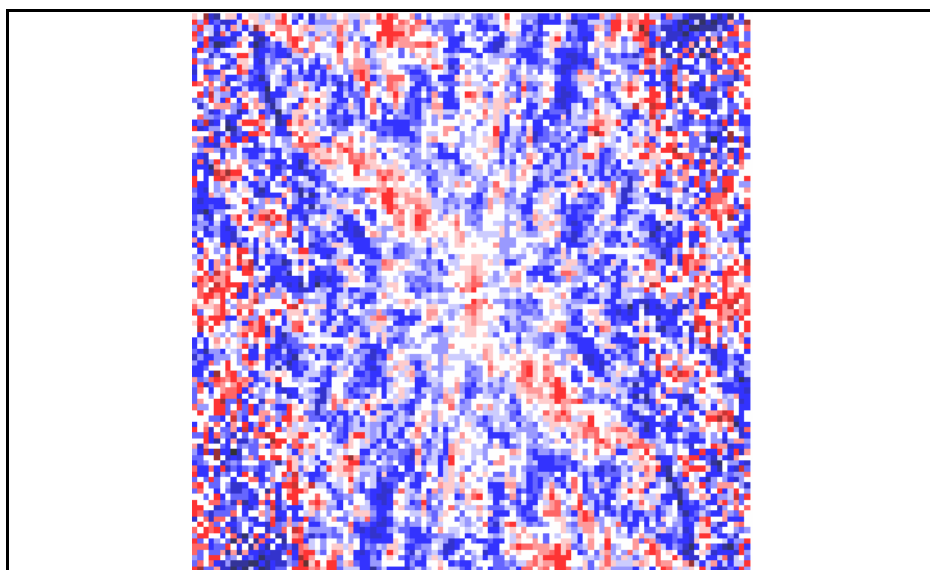
Broadly, these two images appear similar, as they suffer from the same problem as Moran's I lag diagrams as representations of high frequency texture. They do however demonstrate the high degree of scale dependence of the measure, which ranges from order 10 at the lowest lags to order 10,000 at the largest lags. To investigate differences in texture the central portion of the two images was enlarged and the percentage difference in contrast between the two was calculated (something that is easily accomplished in a raster GIS environment). Figure 6.15a shows the scaled difference between the contrast values of the fractal surface and its smoother equivalent with 1/8th of the Fourier coefficients. Figure 6.15b shows a similar difference map

between the fractal and its equivalent surfaces with 1/4 of the Fourier coefficients. Both images show lags of up to 12 raster cells (17 along diagonals).



The difference map shows that proportionally, the greatest difference in texture occurs at the highest frequency (as would be expected). More significantly, a spatial resolution can be identified at which this difference becomes significant. A 10% difference occurs at a lag of approximately 4 raster units in Figure 6.15a and 2 raster units in Figure 6.15b. This corresponds with the doubling of Fourier coefficients between the two surfaces.

A similar proportional difference map was produced for the Inverse Distance Moment measure and is shown in Figure 6.16. The spatial distribution of difference appears contrasts with Figure 6.15, and does not appear to relate to scale in an obvious way. While demonstrating that the Inverse Distance Moment measures different texture properties to Contrast, it is not clear how its meaning should be interpreted.

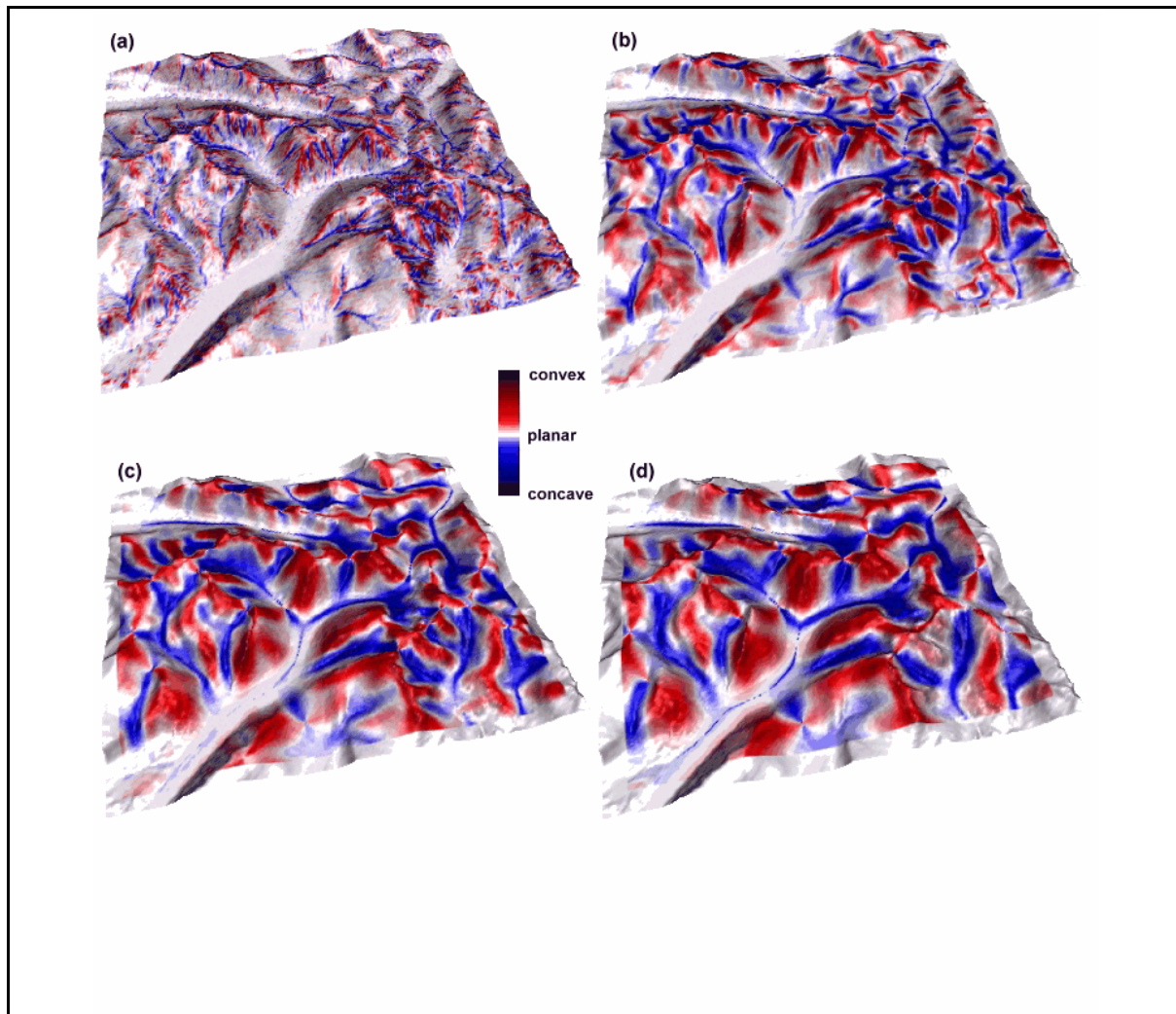


6.5 Terrain Characterisation.

This section describes how the multi-scale characterisation techniques developed can be applied to DEMs representing 'real' terrain. The aim is not to provide a detailed geomorphological analysis, but to demonstrate how, with visual examples, these tools could be used as a mechanism for such analysis. In particular, it is the aim of this section to demonstrate that a multi-scaled characterisation reveals more (useful) information than traditional raster-based geomorphometric analysis.

Figure 6.16 shows the cross-sectional curvature derived from the Lake District DEM at kernel scales of 150m, 450m, 850m and 1.25km. The area represented in the figure is approximately 8 x 8 km with the Wasdale valley in the southwest and the Ennerdale valley running northwest - southeast along the north of the image.

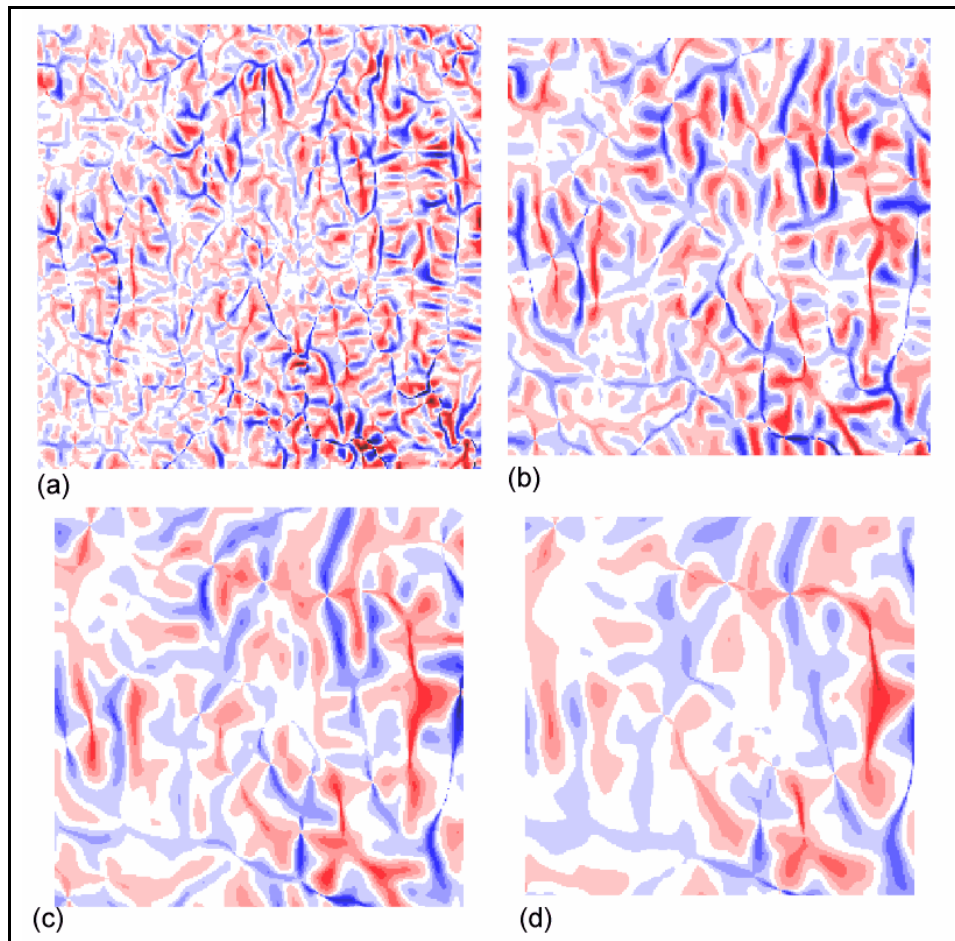
It is clear that the pattern of local curvature varies considerably with scale. At the finest (150m) scale, a rather fragmented network of ridges and channels is revealed. Smaller, well dissected upland valley systems are relatively well defined, while the major valleys are not delineated. Much of the surface is represented as poorly autocorrelated minor concavities and convexities. At a coarser scale, there is far greater spatial autocorrelation in measurement. Figure 6.16d for example shows an almost entirely connected valley network. This suggests that either the true surface varies in roughness with scale (ie not self-similar), or that there is a (random) noise or error component at the highest frequency modelled by the DEM.



The pattern of changing curvature with scale is not symmetrical for concavity and convexity measurements. The 'characteristic scale' beyond which networks are well connected appears to be finer for convexities than for concavities. At the 450m scale (Figure 6.16b), ridges appear well defined while channels systems are represented discontinuously. At the 1.25km scale (Figure 6.16d) channels are still broadly linear features, while surface convexities are in many cases 'spread' over peak features. This asymmetry in pattern is itself a useful diagnostic feature. It is indicative of a glaciated mountain environment previously dominated by erosional processes around ridges and depositional processes along major valley systems.

The animated sequence of changing cross-sectional curvature with scale from which the four images in Figure 6.16 were taken, demonstrates the inadequacy of traditional (single scaled)

raster based measurements. A large valley systems such as Wasdale (southwest of the image) is clearly of some geomorphological importance, yet would not be 'detected' by raster processing at the DEM resolution of 50m. It would seem an unnecessary constraint to consider geomorphological surface variation at one scale alone if a single DEM can reveal pattern over a



range of scales.

Figure 6.17 shows a similar set of cross-sectional curvature values for the Dartmoor region. In this case the kernel size ranges up to 45 x 45 cells (2.3km) over an area of 14km x 14km. As with the Lake District example, the network pattern varies considerably with scale. Again, as with the Lake District, the change in curvature with scale appears asymmetric, but this time, channels are more well defined at finer scales than ridges. It also appears that there is greater spatial variation in convexity with scale than with concavity. This implies the existence of well defined 'V-shaped' channels that are expressed over a range of scales.

The degree to which surface measurements vary with scale was investigated interactively using *d.param.scale* (see Appendix). An indication of scale dependency in morphometric feature classification is shown in Figure 6.18.

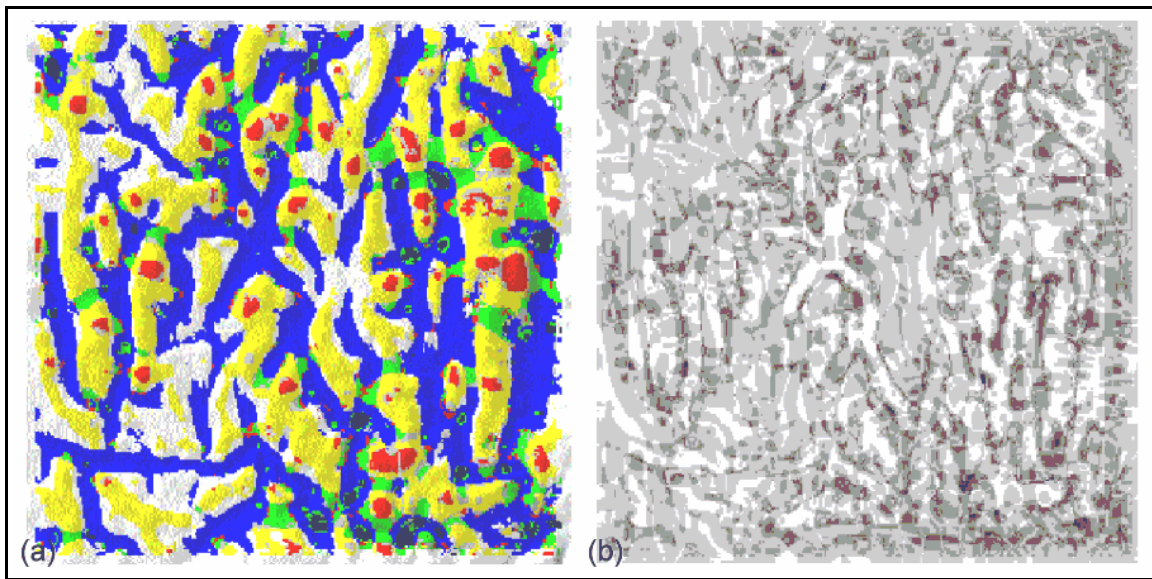
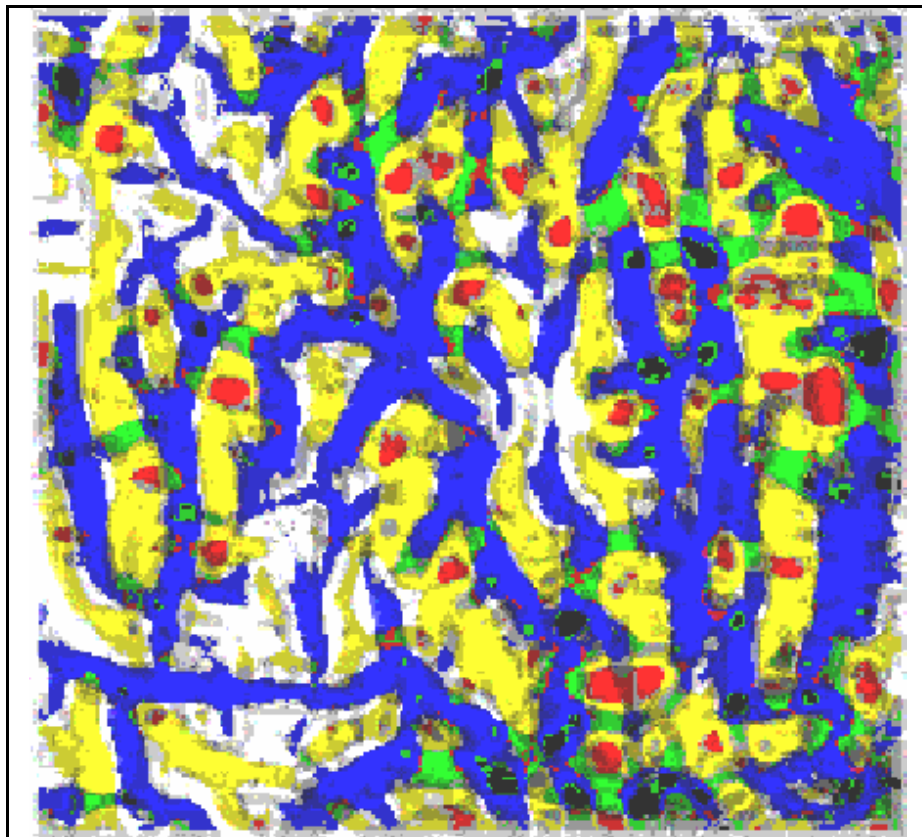
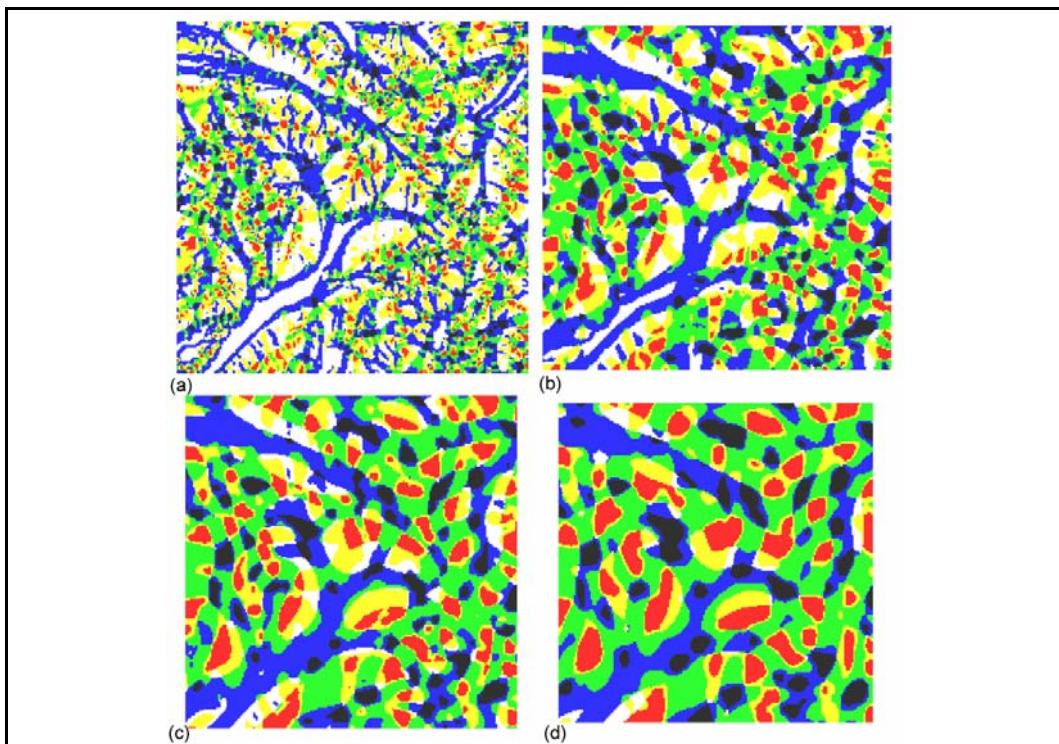


Figure 6.18a displays the most frequent feature classification of each DEM cell based on kernel sizes ranging from 9×9 to 45×45 cells. Where a cell has more than one mode, it is coloured grey. The relationship with relief is emphasised by combining this classification with shaded relief using an hue-intensity mapping. Figure 6.18b shows the confidence with which classification can be made by showing the scaled entropy. The lighter the image, the greater the consistency of feature classification (see section 5.3). These may be combined in a single image using an hue-intensity mapping (Figure 6.19)

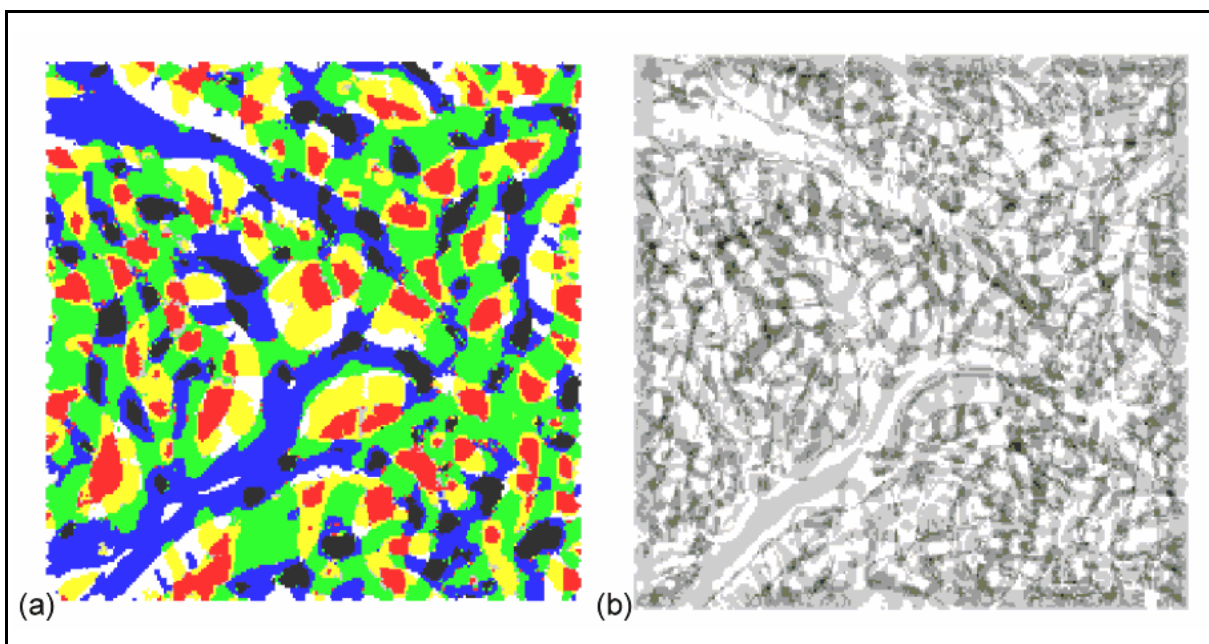


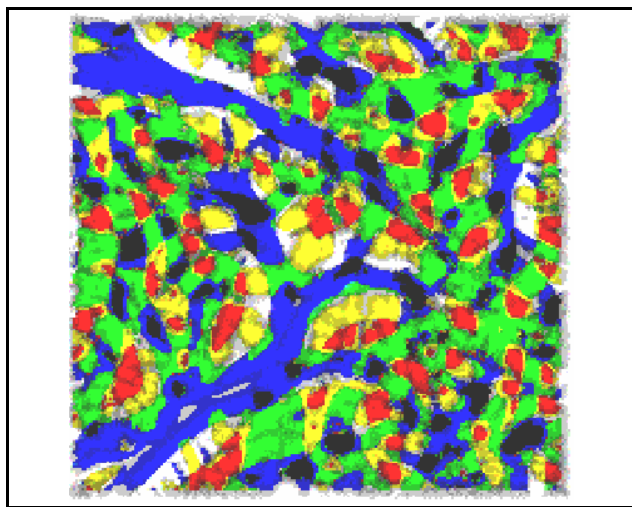
Modal classifications are not all expressed at the same scale. That is, the size of each feature is not consistent over the surface. Features become progressively less well defined towards their edges, as the influence of a wider neighbourhood over a central cell's classification becomes increasingly dominant.

Figure 6.20 shows the scale dependency of feature classification for the Lake District DEM at four different kernel sizes. The slope and curvature tolerance values selected were 20 degrees and 2 respectively.

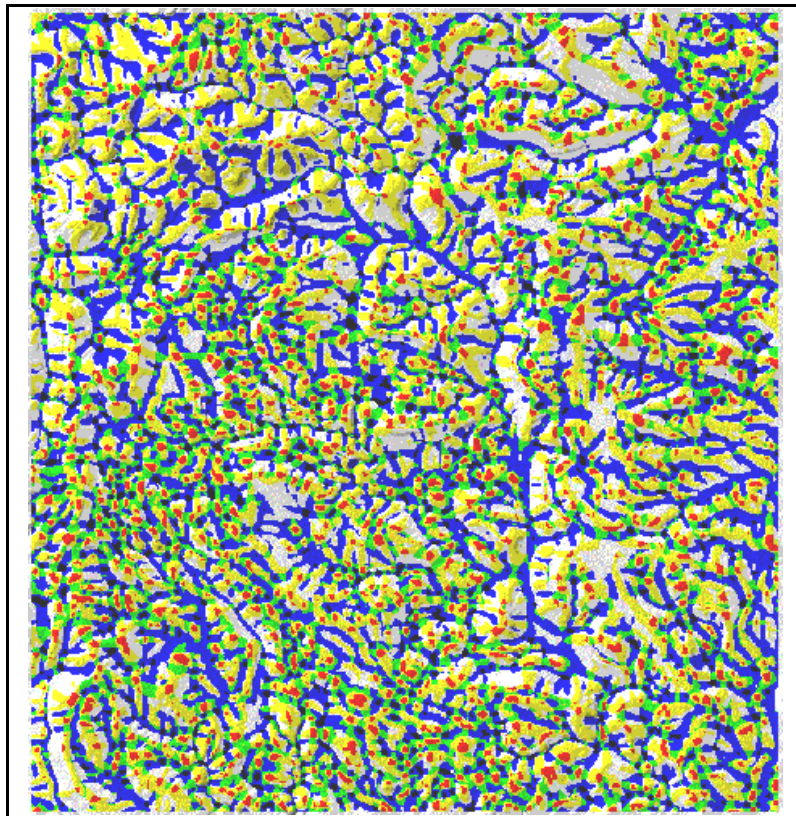


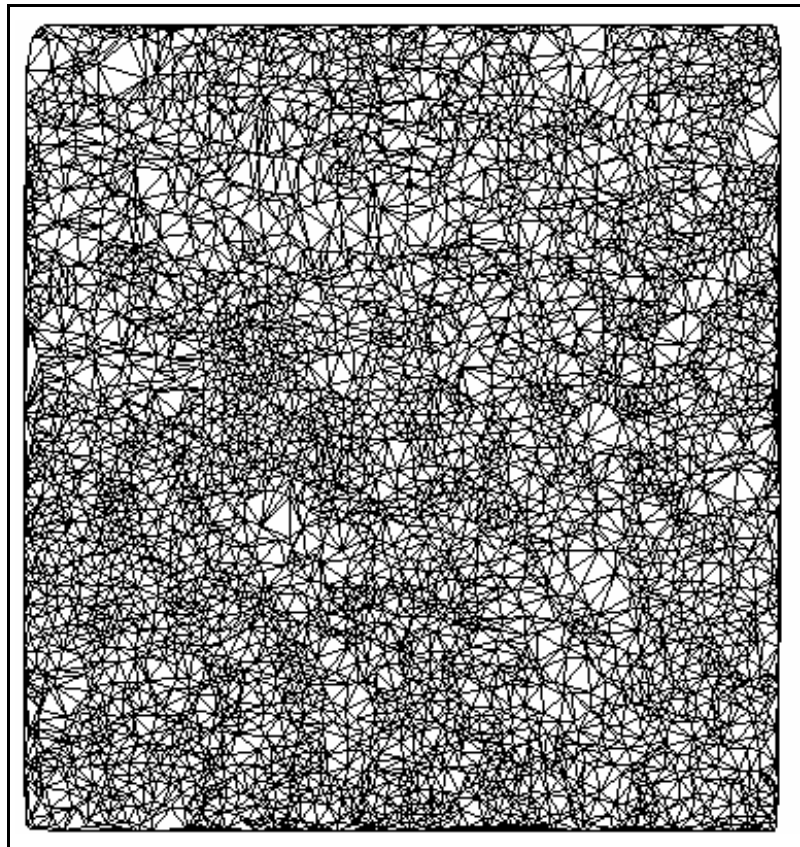
The certainty of feature classification is shown in Figures 6.21 and 6.22 using the mode and entropy method discussed in section 5.3.





One final example of feature classification is provided by the Peak District DEM shown in Figure 6.23. In this case a 15 x 15 cell kernel was passed over the 780 x 800 cell DEM. The distribution of peaks in particular is not uniform of the entire surface, with a higher density of peaks seen to the west and south of the image. This corresponds to the Carboniferous Limestone outcrop which contrasts with the flat topped moorland of Millstone Grit to the north and east. At this scale, the topological relationships between surface features may be of importance. Figure 6.24 shows the Delaunay triangulation of the thinned point features shown in Figure 6.23 (pits, passes and peaks) (see *r.feat.thin* and *v.delaunay* in the Appendix).





Chapter Seven - Conclusions and Further Work.

It has been the aim of this study to develop a new set of tools that describe landscape form. In particular, the *thesis* argued is that this can only be achieved effectively by (i) identifying spatial and scale based variation, and (ii) visualising such variation. This concluding chapter considers the success of the approach by re-evaluating the research objectives stated in the introduction, identifying weaknesses of the approach, and avenues for future research.

7.1 Re-evaluation of Research Aims and Objectives

To assess whether a DEM alone contains useful information for geomorphological characterisation.

This research has been deliberately confined to the analysis of regular matrices of elevation values. Clearly, additional sources of information such as those provided by satellite imagery, and ground survey, provide a more detailed model of landscape. Yet it has been made clear by this work that DEMs are highly information rich descriptions of surface form. It has been argued, that many of the previous attempts to extract information from DEMs have failed to utilise fully, the scale based information contained within the model.

By adopting the parameterisation of surface form first suggested by Evans (1972) it has been possible to examine and quantify local spatial variation systematically. This local description of morphology is sufficiently exhaustive to describe geomorphological form, whilst being sufficiently simple to relate to geomorphological process. Parameterisation has been extended by modelling over a range of scales that remove the surface model from the constraints implied by the DEM resolution. Thus it has been possible to create a more useful source of information for geomorphological analysis.

To identify weaknesses in existing methods of surface characterisation and present new methods to overcome these weaknesses.

The original form of geomorphometric analysis presented by Evans (1972) involved characterisation by quantifying the frequency distribution of surface parameters. Whilst this undoubtedly reveals important diagnostic information, it does little to characterise either the spatial distribution of parameters, or their scale dependency. Quantifications of scale dependencies such as Moran's I spatial autocorrelation index provide little extra information if they are used as a global summary statistic. The solution to this problem suggested by this work is that surface analysis is most effectively carried out within an interactive visualisation context. Consequently, many of the characterisation tools developed have been orientated towards visual representation rather than numerical summary.

More recent geomorphometric analysis has been within the context of the widespread use of Geographical Information Systems. In particular, much research has been devoted to the extraction of hydrological information from DEMs. One of the most significant problems accompanying much of this research has been the apparent mismatch between our own geomorphological understanding of a landscape, and that implied by the raster data model. The multi-scaled parameterisation approach developed here reduces the impact that data model has on subsequent analysis.

To assess the effect that elevation model uncertainty has on surface characterisation.

Two reasons have been identified for the mismatch between true topographic surface form, and its representation as a DEM within a Geographical Information System. Firstly, the model itself provides some conceptual limitations. It is not possible to represent fully, a continuous, undifferentiable surface with a discrete, finite resolution elevation model. Secondly, the process of elevation interpolation required for DEM generation can lead to model error.

It has been demonstrated that the spatial manifestation of DEM error can, in many circumstances, be detected in much the same way as true geomorphometric variation. The

visualisation of hypsometric distributions demonstrated in Chapter 3, has led to the quantification of the terracing effects resulting from contour interpolation. The visualisation of first and second derivatives of interpolated surfaces has allowed the causes of interpolation error to be hypothesised. Visualising the spatial distribution of DEM error has facilitated the development of a deterministic error model based on planimetric offset of elevation data.

These processes have demonstrated that much the same procedure can be adopted when assessing the surface form that is a function of DEM error, and surface form that is a function of geomorphological process. Yet they have also allowed the two to be separated; error possessing a 'topographic signature' in much the same way as geomorphometry. DEM error has been shown empirically to be largely a high frequency phenomenon (usually over a scale of order 1-5 cells) often possessing artifacts of the original data source. Once surface variation is considered at a scale beyond that implied by the DEM resolution, error effects are minimised.

To assess the effectiveness of visualisation as a means of conveying information on surface form, and as a methodological process.

It has been argued that visualisation has been a necessary step in generating the ideas discussed in this study. The interactive generation of images within a GIS environment has allowed ideas to be hypothesised, tested and confirmed. It was used to hypothesise sources of contour interpolation error and to develop a deterministic error model.

Visualisation has been used to illustrate statistical properties of spatial association in the form of lag diagrams. Such patterns would have been revealed by numerical summary alone. Visualisation has been used as a mechanism for conveying complex multivariate information that could not be effectively achieved by other means. The construction of animated sequences (displayed here as *small multiples*) of feature classification patterns changing with scale, simultaneously convey the interrelationship between four geomorphometric quantities (altitude, local relief, feature classification and scale dependency).

To produce working software that may be used in a GIS environment for surface

characterisation.

The appendix to this volume includes the C source code for all software developed for this study. All modules are fully integrated with the GRASS GIS, allowing the benefits of existing GIS technology to be combined with the multiscale visualisation approach suggested here.

7.2 Further Work

7.2.1 Application

Although tools for geomorphometrical analysis have been developed as part of this study, they have not been used to provide a comprehensive or thorough geomorphological assessment of landscape. For the methodology suggested here to be of any use, it must allow new insights into surface form, rather than being used in a confirmatory context. This can only be achieved by considering the geomorphological context more thoroughly.

Multiscale parameterisation has been used to characterise population density surface properties (Wood *et al*, 1996). The use of quadratic generalisation appears particularly appropriate for such surfaces that exhibit a low spatial autocorrelation and strongly positive skew. The use of lag diagrams would be appropriate for analysing surfaces that exhibit anisotropic structural properties over a variety of scales. The rippling of fine grained channel bed form, or larger scale dune systems should be readily detectable using this method.

Work is being carried out in using multi-scaled feature classification as part of the modelling cognitive landscape evaluation. The ability to alter the scale at which features are classified makes this a particularly appropriate approach. A similar classification could be used as part of an automated cartographic generalisation process, both of landscape form and cartographic name placement.

7.2.2 Textural Analysis and Lag Diagrams.

One of the weaknesses in the use of textural lag diagrams was the difficulty in relating the measures with known geomorphological characteristics. It might be more appropriate to use the co-occurrence matrix as the basis for inferential hypothesis testing. The co-occurrence matrix has the form of a contingency table used for categorical data analysis. It would be useful to compare the matrix model with some expectation. Yet the standard Chi-squared expectation of independence is highly artificial for such a spatial distribution. Log-linear modelling provides a mechanism for alternative assumptions to be made about expectations. It would be useful to incorporate models of positive spatial autocorrelation into calculations of model expectation so that it would be possible distinguish 'expected' from 'unexpected' surface behaviour.

7.2.3 Data Structure Development

One of the important results to come from the feature classification process is that a simple Boolean classification of landscape features is not always appropriate. A feature membership function that describes the variation in classification with scale gives a more flexible alternative. Equally, a similar function could describe the change in any morphometric parameter with scale. It would be useful to incorporate such a function into subsequent GIS operations. Fuzzy logic would seem to provide a convenient mechanism for formalising the manipulation of such functions as part of a new type of elevation model.

An alternative elevation model could be developed based on the topological characteristics derived from multiscale quadratic modelling. In particular, the graph theoretic approach suggested by Wolf (1984) provides a parsimonious 'map' of the connectedness of surface features. It is possible to thin point features (ie pits, peaks, passes) and connect with thinned line features (ridges and valleys) as part of a weighted surface network. Such a model could itself be a useful surface characterisation, or alternatively be used for terrain generalisation.

Bibliography

- Abrahams, A. D.** (1984). Channel networks: A geomorphological perspective. *Water Resources Research*. 20 (2), 161-168.
- Ackermann, F.** (1993) Automatic generation of digital elevation models, 16 pp. *presented at OEEPE Commision B, DTM Accuracy Meeting, Southampton.*
- Ammeraal, L.** (1986) *Programming Principles in Computer Graphics*, London: Wiley.
- Bailey, T. and Gatrell, A.** (1995) *Interactive Spatial Data Analysis*, Essex: Longman
- Bajcsy, R.** (1973) Computer description of textured surfaces, *Proceedings, 1973 International Conference on Artificial Intelligence*, pp.572-579
- Band, L.E.** (1989) A terrain based watershed information system. *Hydrological Processes* 3, pp.151-162
- Band, L. E.** (1986). Topographic partition of watersheds with digital elevation models. *Water Resources Research* 22(1), pp.15-24.
- Band, L. E. and Wood, E. F.** (1988). Strategies for large scale, distributed hydrologic simulation. *Applied Mathematics and Computation*. 27, pp.33-37.
- Barnsley, M.F.** (1988) *Fractals Everywhere*, Academic Press.
- Bathurst, J.C.** (1986) Physically-based distributed modelling of an upland catchment using the Systeme Hydrologique Europeen, *Journal of Hydrology*, 87, pp.79-102.
- Beard, M.K., Buttenfield, B.P., and Clapham, S.B.** (1991) NCGIA research initiative 7: Visualisation of spatial data quality, *Technical Paper 91-26*, National Center for Geographic Information and Analysis, Santa Barbara
- Bennett, D. A. and Armstrong, M. P.** (1989). An inductive bit-mapped classification scheme for terrain feature extraction. *Proceedings of the GIS/LIS conference 1989, Orlando*. 1, pp.59-68.
- Brassel, K.** (1974) A model for automatic hill shading. *The American Cartographer* 1(1), pp. 15-27
- Brown, D.G. and Bara, T. J.** (1994) Recognition and reduction of systematic error in elevation and derivative surfaces from 7 1/2 minute DEMs, *Photogrammetric Engineering and Remote Sensing*, 60 (2), pp.189-194.
- Burrough, P.A.** (1981) Fractal dimensions of landscapes and other environmental data. *Nature*, 294, pp.240-242.

- Burrough, P.A.** (1986) *Principles of Geographical Information Systems for Land Resources Assessment*. OUP, Oxford, Ch.8, Methods of interpolation, pp. 147-166.
- Burrough, P.A.** (1993) Fractals and geostatistical methods in landscape studies, in **Lam, N. and De Cola, L.** *Fractals in Geography*, Englewood Cliffs, NJ: Prentice Hall.
- Burrough, P.A. and Heuvelink, G.B.M.** (1992) The sensitivity of Boolean and continuous (fuzzy) logical modelling to uncertain data. *Proceedings, EGIS 92, Munich 2*, pp.1032-1041
- Carter, J.R.** (1989) Relative errors identified in USGS DEMs. *Proceedings, Auto Carto 9*, American Congress on Surveying and mapping, Bethesda, Maryland, pp.255-265
- Carter, J.** (1992) The effect of data precision on the calculation of slope and aspect using gridded DEMs, *Cartographica*, 29 (1), pp.22-34.
- Cayley, A.** (1859). On contour and slope lines. *The London, Edinburgh, and Dublin Philosophical Magazine and Journal of Science*. XVIII, pp. 264-268.
- CERL** (1991) The GRASS 4.0 Reference Manual. U.S. Army Construction Engineering Research Laboratory, Champaign, Illinois.
- Chambers** (1990) *Chambers English Dictionary*, 7th Edition, Edinburgh: Chambers.
- Chang, K. and Tsai, B.** (1991) The effect of DEM resolution on slope and aspect mapping, *Cartography and Geographic Information Systems*, 18, pp.69-77.
- Chrisman, N.R.** (1989) Modeling error in overlaid categorical maps. in **Goodchild, M.F. and Gopal, S.** (eds.) (1989) *The Accuracy of Spatial Databases*. Taylor and Francis, London. pp.21-34
- Chorley, R.J., Malm, D.E. and Pogorzelski, H.A.** (1957) A new standard for estimating drainage basin shape, *American Journal of Science*, 255(2) pp.138-141.
- Chorowicz, J., Ichoku, C., Raizanoff, S., Kim, Y., and Cervelle, B.** (1992) A combined algorithm for automated drainage network extraction, *Water Resources Research*, 28 (5), pp.1293-1302.
- Chorowicz, J., Kim, J., Manoussis, S., Rudant, J., Foin, P. and Veillet, I.** (1989) A new technique for recognition of geological and geomorphological patterns in digital terrain models, *Remote Sensing of Environment*, 29 (3), pp.229-239.
- Church, M. and Mark, D.** (1980) On size and scale in geomorphology, *Progress in Physical Geography* 4, pp.342-390

- Clarke, K.C.** (1986) Computation of the fractal dimension of topographic surfaces using the triangular prism surface area method, *Computers and Geosciences*, 12 (5), pp.713-722.
- Clarke, K. C.** (1988). Scale based simulation of topographic relief. *The American Cartographer* 15 (2), pp.171-181.
- Clarke, K., and Schweitzer, D.** (1991) Measuring the fractal dimension of fractal surfaces using a robust fractal estimator, *Cartography and Geographic Information Systems*, 18 (1)
- Cliff, A.D. and Ord, J.K.** (1981) *Spatial Processes, Models and Applications*, London: Pion.
- Collins, S. H.** (1975). Terrain parameters directly from digital elevation models. *Canadian Surveyor* 29 (5), pp.507-518.
- Cressie, N.A.C.** (1993) *Statistics for Spatial Data*. Ney York: Wiley.
- Culling, W.E.H.** (1989) The characterization of regular/irregular surfaces in the soil-covered landscape by gaussian random fields, *Computers and Geosciences*, 15 (2), pp.219-226.
- Darling, E. and Joseph, R.** (1968) Pattern recognition from satellite altitudes, *IEEE Transactions on Systems, Science and Cybernetics*, 4, pp.38-47.
- Datcu, M. and Seidel, K.** (1995) Fractal and multi-resolution techniques for the understanding of geo-information, in **Wilkinson, G, Kanellopoulos, I. and Mégier, J.** (eds) *Fractals in Geosciences and Remote Sensing*, Joint Research Centre, Report EUR 16092 EN. pp.56-84
- DiBiase, D.** (1990) Visualisation in the earth sceinces, *Earth and Mineral Sciences, Pennsylvania State University*, 59(2), pp.13-18.
- Dietler, G.** (1995) The fractal structure of materials and surfaces, in **Wilkinson, G, Kanellopoulos, I. and Mégier, J.** (eds) *Fractals in Geosciences and Remote Sensing*, Joint Research Centre, Report EUR 16092 EN. pp.325-341.
- Dietler, G. and Zhang, Y.** (1992) Fractal aspects of the Swiss landscape, *Physica A*, 191, pp.213-219.
- Dikau, R.** (1989) The application of a digital relief model to landform analysis in geomorphology. in *Three dimensional applications in GIS*, **Raper, J.** ed., Taylor and Francis, London, pp.51-77
- Doornkamp, J.C.** (1968) The analysis of the morphometric properties of drainage basins by the Spearman's rank correlation technique, in **Slaymaker, H.O. (ed)** (1968) Morphometric analysis of maps, *British Geomorphological Research Group, Occasional Paper*, pp.31-40.

- Douglas, D. H.** (1986). Experiments to locate ridges and channels to create a new type of digital elevation model. *Cartographica* 23(1), pp.29-61.
- Dunkerley, D. L.** (1977). The frequency distributions of stream link lengths and the development of channel networks. *Journal of Geology*, 1985, pp.459-470.
- Dury, G.H.** (1951) Quantitive measurement of available relief and depth of dissection, *Geological Magazine*, 88(5), pp.339-343.
- Dykes, J.A.** (1994) Area-value data: New visual emphases and representations. in **Hearnshaw and Unwin (eds)** (1994) *Visualization in Geographical Information Systems*, Chichester: Wiley, pp.103-114
- Evans, I. S.** (1972). General geomorphometry, derivatives of altitude, and descriptive statistics. in **Chorley, R. J.** ed. *Spatial Analysis in Geomorphology*, Methuen, London. pp.17-90.
- Evans, I.S.** (1979) An integrated system of terrain analysis and slope mapping. *Final report on grant DA-ERO-591-73-G0040*, University of Durham, England.
- Evans, I.S.** (1980) An integrated system of terrain analysis and slope mapping. *Zeitschrift fur Geomorphologie*, Suppl-Bd 36, pp.274-295.
- Evans, I.S.** (1981) General geomorphometry, in **Goudie, A.S.** (ed.), *Geomorphological Techniques*, pp.31-37.
- Evans, I.S.** (1984) Correlation structures and factor analysis in the investigation of data dimensionality: statistical properties of the Wessex land surface, England, *International Symposium on Spatial Data Handling*, Zurich, 1, pp.98-116.
- Fairfield, J. and Leymarie, P.** (1991) Drainage networks from grid digital elevation models, *Water Resources Research*, 27(5), pp.709-717.
- Feder, J.** (1988) *Fractals*, Plenum Press.
- Frederiksen, P., Jacobi, O., and Kubik, K.** (1984) Modelling and classifying terrain, *International Archives of Photogrammetry and Remote Sensing*, XXV, Part A3a, pp.256-257.
- Fioravanti, S.** (1995) Multifractals: theory and application to image texture recognition, in **Wilkinson, G., Kanellopoulos, I. and Mégier, J.** (eds) *Fractals in Geosciences and Remote Sensing*, Joint Research Centre, Report EUR 16092 EN. pp.152-175
- Fisher, P.F.** (1990) Simulation of error in digital elevation models. *Papers and Proceedings of the 13th Applied Geography Conference* 13, pp. 37-43

- Fisher, P.F.** (1991a) Modelling soil map-unit inclusions by Monte Carlo simulation, *International Journal of Geographical Information Systems*, 5(2), pp.192-208.
- Fisher, P.F.** (1991b) First experiments in viewshed uncertainty: The accuracy of the viewshed area. *Photogrammetric Engineering and Remote Sensing* 57 (10) pp.1321-1327
- Fisher, P.F.** (1992) First experiments in viewshed uncertainty: Simulating fuzzy viewsheds. *Photogrammetric Engineering and Remote Sensing* 58 (4) pp.345-352
- Fisher P.** (1993) Algorithm and implementation uncertainty in viewshed analysis, *International Journal of Geographical Information Systems*, vol 7 (4) pp.331-347
- Fox, C.G.** (1989) Empirically derived relationships between fractal dimension and power law form frequency spectra, *Pure and Applied Geophysics*, 131 (1/2) pp.211-239.
- Frank, A., Palmer, B. and Robinson, V.** (1986) Formal methods of the accurate definition of some fundamental terms in physical geography, *Proceedings, Second International Symposium on Spatial Data Handling, Seattle*, pp.583-599.
- Gallant, J.C. and Hutchinson, M.F.** (1996) Towards an understanding of landscape scale and structure, *Proceedings, Third International Conference on Integrating GIS and Environmental Modelling*, http://www.ncgia.ucsb.edu/conf/santa_fe.html, Santa Barbara: National Center for Geographic Information and Analysis
- Garbrecht, J. and Martz, L.** (1993) Grid size dependency of parameters from digital elevation models, 12 pp. (source unknown)
- Garbrecht, J. and Starks, P.** (1995) Note on the use of USGS level 1 7.5-minute DEM coverages for landscape drainage analyses, *Photogrammetric Engineering and Remote Sensing*, 61 (5), pp.519-522.
- Gardner, T.W., Sasowsky, K.C., and Day, R.L.** (1990) Automated extraction of geomorphometric properties from digital elevation data, *Zeitschrift fur Geomorphologie Suppl.* 80, pp.57-68.
- Gilbert, L. E.** (1989) Are topographic data sets fractal ? *Pure and Applied Geophysics*, 131(1/2), pp.241-254.
- Glock, W.S.** (1932) Available relief as a factor of control in the profile of a land form, *Journal of Geology*, 40(1), pp.74-83.
- Gonzalez, R. C. and Woods, R.C.** (1992) *Digital Image Processing*, Reading, Mass: Addison-Wesley.
- Goodchild, M.F.** (1980) Fractals and the accuracy of geographical measures, *Mathematical Geology* 12(2), pp.85-98

- Goodchild, M.F.** (1982) The fractional Brownian process as a terrain simulation model, *Modelling and Simulation*, 13, pp.1133-1137.
- Goodchild, M. F.** (1986) Spatial Autocorrelation, *Concepts and Techniques in Modern Geography (CATMOG)* 47, GeoBooks, Norwich.
- Goodchild, M. F.** (1988). Lakes on fractal surfaces: A null hypothesis for lake-rich landscapes. *Mathematical Geology* 20,6, pp.615-630.
- Goodchild, M.F. and Grandfield, A.W.** (1983) Optimizing raster storage: An evaluation of four alternatives, *Proceedings, Sixth International Symposium on Automated Cartography, Ottowa (Auto-Carto VI)*, 2, pp.400-407.
- Goodchild, M.F. and Gopal, S.** (eds.) (1989) *The Accuracy of Spatial Databases*. Taylor and Francis, London.
- Goodchild, M.F., Guoqing, S. and Shiren, Y.** (1992) Development and test of an error model for categorical data. *International Journal of Geographical Information Systems* 6 (2) pp.87-104
- Goodchild, M. F. and Mark, D. M.** (1987). The fractal nature of geographic phenomena. *Annals of the Association of American Geographers* 77(2), pp.265-278.
- Goudie, A.** (1990) (ed) *Geomorphological Techniques (second edition)*, London: Unwin for the British Geomorphological Research Group.
- Gould, P.R.** (1967) On the geographical interpretation of eigenvalues, *Transactions of the Institute of British Geographers*, 42, pp.53-86.
- Govaerts, Y and Verstraete, M.** (1995) Applications of the L-systems to canopy reflectance modelling in a Monte Carlo ray tracing technique in **Wilkinson, G, Kanellopoulos, I. and Mégier, J.** (eds) *Fractals in Geosciences and Remote Sensing*, Joint Research Centre, Report EUR 16092 EN. pp.211-236
- Graff, L.H. and Usery, E.L.** (1993) Automated classification of generic terrain features in digital elevation models, *Photogrammetric Engineering and Remote Sensing*, 59(9), pp.1409-1417.
- Graps, A.** (1995) An introduction to wavelets, *IEEE Computational Science and Engineering*, 2(2), 18 pp.
- Guth, P.** (1992) Spatial analysis of DEM error, *Proceedings, ASPRS/ACSM Annual Meeting, Washington DC*, pp.187-196.
- Haber, R.B. and McNabb, D.A.** (1990) Visualisation idioms: a conceptual model for scientific visualisation systems, in Neilson, M., Shriver, B., and Rosenblbaum, L. (1990)

- Visualisation in scientific computing*, IEEE Computer Society Press.
- Hack, J.T.** (1957) Studies of longitudinal stream profiles in Virginia and Maryland, *US Geological Survey, Professional Paper 294-B*, pp.45-94.
- Haining, R., Griffith, D. and Bennett, R.** (1983) Simulating two-dimensional autocorrelated surfaces, *Geographical Analysis*, 15(3), pp.247-255
- Hakanson, L.** (1978) The length of closed geomorphic lines, *Mathematical Geology* 10, pp.141-167.
- Hannah, M.J.** (1981) Error detection and correction in digital terrain models. *Photogrammetric Engineering and Remote Sensing* 47(1), pp.63-69.
- Haralick, R.M., Shanmugam, K. and Dinstein, I.** (1973) Textural features for image classification. *IEEE Transactions on Systems, Man, and Cybernetics*, 3(6), pp.610-611.
- Haralick, R.M.** (1979) Statistical and structural approaches to texture, *IEEE Transactions on Systems, Man and Cybernetics*, 4(7), pp.394-396.
- Haralick, R.M.** (1983) Ridge and valley on digital images, *Computer Vision, Graphics and Image Processing*, 22(1), pp.28-38.
- Heerdegen, R.G. and Beran, M.A.** (1982) Quantifying source areas through land surface curvature and slope, *Journal of Hydrology*, 57 (3-4), pp.359-373.
- Heuvelink, G.B.** (1993) *Error Propagation in Quantitative Spatial Modelling. Applications in Geographical Information Systems*, University of Utrecht.
- Hodgson, M.E.** (1995) What cell size does the computed slope / aspect angle represent ? *Photogrammetric Engineering and Remote Sensing*, 61(5), pp. 513-517.
- Horton, R.E.** (1945) Erosional development of streams and their drainage basins, hydrophysical approach to quantitative morphology, *Bulleting, Geological Society of America*, 56(3), pp.275-370.
- Huang, J. and Turcotte, D.** (1989) Fractal mapping of digitized images - application to the topography of Arizona and comparisons with synthetic images, *Journal of Geophysical Research* 94 (B6), pp.7491-7495
- Huang, J. and Turcotte, D.** (1990) Fractal image analysis: application to the topography of Oregon and synthetic images, *Journal of the Optical Society of America A*, 7(6), pp.1124-1130
- Hunter, G.J. and Goodchild, M.F.** (1995) Dealing with error in spatial databases: A simple case study, *Photogrammetric Engineering and Remote Sensing*, 61(5), pp.529-537.

- Hurst, H., Black, R., and Simaika, Y.** (1965) *Long-Term Storage: An Experimental Study*, London: Constable.
- Hutchinson, M.F.** (1989). A new procedure for gridding elevation and stream line data with automatic removal of spurious pits. *Journal of Hydrology* 106, pp.211-232.
- Imhof, E.** (1982) *Cartographic Relief Presentation*, (ed Steward, H.J), Berlin: Walter de Gruyter.
- Isaaks, E.H. and Srivastava, R.M.** (1989) *An Introduction to Applied Geostatistics*, Oxford: Oxford University Press.
- Jarvis, R.S.** (1981) Specific geomorphometry, in **Goudie, A.S.** (ed.), *Geomorphological Techniques*, pp.42-46.
- Jarvis, R. S. and Sham, C. H.** (1981). Drainage network structure and the diameter magnitude relation. *Water Resources Research*. 17, pp.1019-1027.
- Jenson, S. K.** (1985). Automated detection of hydrologic basin characteristics from digital elevation model data. *Digital Representation of Spatial Knowledge, Auto-Carto 7., American society of Photogrammetry and the American Congress on Surveying and Mapping*. pp.301-310.
- Jenson, S.K.** (1991) Applications of hydrologic information automatically extracted from digital elevation models, *Hydrological Processes* 5, pp.31-44.
- Jenson, S. K. and Domingue, J. O.** (1988). Extracting topographic structure from digital elevation data for geographic information system analysis. *Photogrammetric Engineering and Remote Sensing* 54(11), pp.1593-1600.
- Johnson, D.** (1933) Available relief and texture of topography, a discussion, *Journal of Geology*, 41(3), pp.293-305.
- de Jong, S.** (1995) Mapping Spatial Variability in Landscapes: An example using fractal dimensions, in **Wilkinson, G., Kanellopoulos, I. and Mégier, J.** (eds) *Fractals in Geosciences and Remote Sensing*, Joint Research Centre, Report EUR 16092 EN. pp.176-210.
- Kaizer, H.** (1955) A quantification of textures on aerial photographs, *Technical Note 121, AD 69484, Boston University Research Laboratory*.
- Kidner, D.B., Jones, C.B., Knight, D.G. and Smith, D.H.** (1990) Digital terrain models for radio path profiles. *Proceedings of the 4th International Symposium on Spatial Data*

Handling, Zurich, pp.240.

King, C.A. (1968) A morphometric example of factor analysis in **Slaymaker, H.O. (ed)** (1968) Morphometric analysis of maps, *British Geomorphological Research Group, Occasional Paper*, pp.41-48.

Klinkenberg, B. (1992) Fractals and morphometric measures: is there a relationship ? *Geomorphology* 5, pp.5-20

Klinkenberg, B. and Goodchild, M. (1992) The fractal properties of topography: A comparison of methods, *Earth Surface Processes and Landforms*, 17, pp.217-234.

Knighton, A.D. (1984) *Fluvial Forms and Processes*, London: Arnold.

Kumler, M.P. (1994) An intensive comparison of triangulated irregular networks (TINs) and Digital Elevation Models (DEMs), *Cartographica, Monograph*, 31(2).

Lam, N. (1983) Spatial Interpolation methods: A review, *American Cartographer*, 10, pp.129-149.

Lam, N. and De Cola, L. (1993) *Fractals in Geography*, Englewood Cliffs, NJ: Prentice Hall

Lammers, R. and Band, L. (1990) Automating object representation of drainage basins, *Computers and Geosciences*, 16 (6), pp. 787-810

Lavalle, D., Lovejoy, S., Schertzer, D. and Ladoy, D. (1993) Non-linear variability in landscape topography: Multifractal analysis and simulation, in **Lam, N. and De Cola, L. (eds)** *Fractals in Geography*, Englewood Cliffs, NJ: Prentice Hall

Lee, J., Snyder, P.K. and Fisher, P.F. (1992) Modelling the effect of data errors on feature extraction from digital elevation models. *Photogrammetric Engineering and Remote Sensing* 58(10) pp.1461-1467

Lévy-Véhel, J. (1995) Multifractal analysis of remotely sensed images, in **Wilkinson, G., Kanellopoulos, I. and Mégier, J. (eds)** *Fractals in Geosciences and Remote Sensing*, Joint Research Centre, Report EUR 16092 EN, pp.85-101.

Lewis, L.A. (1968) Analysis of surficial landform properties-the regionalization of Indiana into units of morphometric similarity, *Proceedings of the Indiana Academy of Science*, 78, pp.317-328.

Li, Z. (1988) On the measure of digital terrain model accuracy. *Photogrammetric Record*, 72 (12), pp.873-877.

Li, Z. (1993a) Theoretical models of the accuracy of digital terrain models: An evaluation and

- some observations, *Photogrammetric Record* 14 (82), pp.651-659.
- Li, Z. (1993b)** Mathematical models of the accuracy of digital terrain model surfaces linearly constructed from square gridded data, *Photogrammetric Record* 14 (82), pp.661-673.
- Lifton, N.A. and Chase, C.G. (1992)** Tectonic, climatic, and lithologic influences on landscape fractal dimension and hypsometry: Implications for landscape evolution in the San Gabriel mountains, California, *Geomorphology* 5, pp.77-114.
- Lovejoy, S. and Schertzer, D. (1995)** How bright is the coast of Brittany ?, in **Wilkinson, G, Kanellopoulos, I. and Mégier, J. (eds)** *Fractals in Geosciences and Remote Sensing*, Joint Research Centre, Report EUR 16092 EN. pp.102-151
- Lu, S.Y. and Fu, K.S. (1978)** A syntactic approach to texture analysis, *Computer Graphics and Image Processing*, 7(3), pp.303-330
- MacEachren, A.M. and Davidson, J.V. (1987)** Sampling and isometric mapping of continuous geographic surfaces. *The American Cartographer* 14,(4) pp.299-320.
- Mackaness, W. and Beard, K. (1993)** Use of graph theory to support map generalisation, *Cartography and Geographical Information Systems*, 20(4), pp.210-221.
- McLaren, R.A., and Kennie, T.J.M. (1989)** Visualisation of digital terrain models: techniques and applications. in *Three dimensional applications in GIS*, **Raper, J.** ed., Taylor and Francis, London, pp.80-98
- Mandelbrot, B.B (1967)** How long is the coastline of Britain ? Statistical self-similarity and fractional dimension, *Science* 156, pp.636-638.
- Mandelbrot, B.B. (1975)** *Les Objects Fractal: Forme, Hasard et Dimension*, Paris: Flammarion
- Mandelbrot, B.B. (1977)** *Fractals: Form, Chance and Dimension*, San Fransisco: WH Freeman
- Mandelbrot, B.B. (1982)** *The Fractal Geometry of Nature*, New York: WH Freeman
- Mandelbrot, B.B. (1986)** Self-affine fractal sets, in **Pietronero, L. and Tosatti, E.** (eds) *Fractals in Physics*, Holland, pp.3-28
- Mark, D.M. (1975a)** Geomorphometric parameters: a review and classification, *Geografiska Annaler* 57 A, pp.165-177.
- Mark, D.M. (1975b)** Computer analysis of topography: a comparison of terrain storage methods, *Geografiska Annaler* 57 A, pp.179-188.
- Mark, D.M. (1979)** Topology of ridge patterns, randomness and constraints, *Bulletin*,

Geological Society of America, 90(2) pp.164-172.

Mark, D. M. (1983a). Automated detection of drainage networks from digital elevation models. in: **Wellar, B. S.** 1983 . *Automated Cartography: international perspectives on achievements and challenges. Ottawa, Auto-Carto Six 2, pp.168-177.*

Mark, D. M. (1983b). Relations between field-surveyed channel networks and map-based geomorphometric measures, Inez, Kentucky. *Annals of the Association of American Geographers. 73, pp.358-272.*

Mark, D. M. and Aronson, P.B. (1984) Scale-Dependent fractal dimensions of topographic surfaces: An empirical investigation with applications in geomorphology and computer mapping, *Mathematical Geology, 16 (7), pp.671-683.*

Marks, D., Dozier, J. and Frew, J. (1983). Automated basin delineation from digital terrain data. *NASA Technical Memorandum 84984.*

Martz, L.W. and DeJong, E. (1988) Catch: A Fortran program for measuring catchment area from digital elevation models, *Computers and Geosciences, 14(5), pp.627-640.*

Martz, L.W. and Garbrecht, J. (1992) Numerical definition of drainage network and subcatchment areas from Digital Elevation Models. *Computers and Geosciences, 18 (6), pp. 747-761*

Maxwell, J.C. (1870). On contour lines and measurements of heights. *The London, Edinburgh and Dublin Philosophical Magazine and Journal of Science. 40, pp.421-427.*

McKim, R.H. (1972) *Experiences in Visual Thinking*, Monterey, CA: Brooks/Cole.

Meisels, A., Raizman, S. and Karnieli, A. (1995) Skeletonizing a DEM into a drainage network, *Computers and Geosciences, 21 (1), pp.187-196.*

Miller, R.L. and Kahn, J.S. (1962) *Statistical Analysis in the Geological Sciences*, John Wiley, London.

Mitasova H. (1992) Surfaces and Modelling, *Grassclippings, The Journal of Open Geographical Information Systems, 6 (3), pp.16-18.*

Mitasova H. and Mitas, L. (1993) Interpolation by regularized spline with tension: I theory and implementation, *Mathematical Geology.*

Monckton, C. (1994) An investigation into the spatial structure of error in digital elevation data, *Innovations in GIS 1, pp.201-211*, London: Taylor and Francis.

- Monkhouse, F.J. and Wilkinson, H.R.** (1952) *Maps and Diagrams: Their Compilation and Construction*. 3rd edition, 1971, London:Methuen
- Moore, I.D., Grayson, R.B. and Ladson, A.R** (1991) Digital terrain modelling: A review of hydrological, geomorphological and biological applications, *Hydrological Processes* 5, pp.3-30.
- Morris, D.G. and Flavin, R.W.** (1984) A digital terrain model for hydrology, *4th International Symposium on Spatial Data Handling, Zurich*, pp.250-262.
- Morris, D.G. and Heerdegen, R.G.** (1988) Automatically derived catchment boundaries and channel networks and their hydrological applications. *Geomorphology 1*, pp.131-141
- O'Callaghan, J. F. and Mark, D. M.** (1984). The extraction of drainage networks from digital elevation data. *Computer Vision, Graphics and Image Processing*. 28, pp.323-344.
- Ohmori, H. and Hirano, M.** (1984) Mathematical explanation of some characteristics of altitude distributions of landforms in an equilibrium state, *Transactions, Japanese Geomorphological Union*, 5(4), pp.293-310.
- Oliver, M., Webster, R. and Gerrard, J.** (1989a) Geostatistics in physical geography. Part I: theory, *Transactions, Institute of British Geographers*, 14, pp.259-269.
- Oliver, M., Webster, R. and Gerrard, J.** (1989b) Geostatistics in physical geography. Part II: applications, *Transactions, Institute of British Geographers*, 14, pp.270-286.
- Onorati, G., Poscolieri, M., Ventura, R., Chiarini, V. and Crucilla, U.** (1992) The digital elevation model of Italy for geomorphology and structural geology, *Catena* 19, pp.147-178.
- Ordnance Survey** (1992) *1:50 000 Scale Height Data User Manual*. Ordnance Survey, Maybush, Southampton.
- Ordnance Survey** (1993) *A Technical Guide for Sample Digital Map Data in National Transfer Format Version 2.0*. Ordnance Survey, Maybush, Southampton.
- Ostman, A.** (1987) Accuracy estimation of digital elevation data banks, *Photogrammetric Engineering and Remote Sensing*, 53 (4), pp.425-430
- Outcalt, S. and Melton, M.** (1992) Geomorphic application of the Hausdorff-Besicovich dimension, *Earth Surface Processes and Landforms*, 17, pp. 775-787.
- Ovenden, J. C. and Gregory, K. J.** (1980) The permanence of stream networks in Britain. *Earth Surface Processes*. 5, pp.47-60.

- Palacois-Velez, O. L. and Cuevas-Renaud, B.** (1986). Automated river-course, ridge and basin delineation from digital elevation data. *Journal of Hydrology* 86, pp.299-314.
- Peitgen, H.O. and Saupe, D.** (1988) (eds) *The Science of Fractal Images*, pp.312, London: Springer-Verlag.
- Pentland, A. P.** (1984) Fractal based description of natural scenes, *IEEE Transactions on Pattern Analysis and Machine Intelligence, PAMI-6* (6), pp.661-674.
- Petrie, G. and Kennie, T.J.** (1990) (eds) *Terrain Modelling in Surveying and Civil Engineering*, Caithness: Whittles.
- Peucker, T.K.** (1978) Data structures for digital terrain models - discussion and comparison, in **Dutton, G. (ed)**, *Harvard Papers on Geographic Information Systems*.
- Peucker, T. K. and Douglas, D. H.** (1974). Detection of surface specific points by local parallel processing of discrete terrain elevation data. *Computer Graphics and Image Processing* 4, pp.375-387.
- Pike, R.J.** (1988) The geometric signature: Quantifying landslide terrain types from digital elevation models, *Mathematical Geology*, 20 (5), pp.491-511.
- Pike, R.J.** (1993) A bibliography of geomorphometry, *United States Geological Survey Open-File Report 93-262-A*, pp. 132, Menlo Park, CA.
- Pfaltz, J. L.** (1976). Surface networks. *Geographical Analysis* 8(1), pp.77-93.
- Polidori, L.** (1995) Fractal-based evaluation of relief mapping techniques, in **Wilkinson, G., Kanellopoulos, I. and Mégier, J. (eds)** *Fractals in Geosciences and Remote Sensing*, Joint Research Centre, Report EUR 16092 EN. pp.277-297.
- Polidori, L. and Chorowicz, J.** (1990) Modelling terrestrial relief with Brownian motion: Application to digital elevation data evaluation and resampling, *EARSeL Symposium, Graz*.
- Polidori, L., Chorowicz, J. and Guillande, R.** (1991) Description of terrain as a fractal surface, and application to digital elevation model quality assessment, *Photogrammetric Engineering and Remote Sensing*, 57 (10), pp.1329-1332
- Press, W.H., Flannery, B.P., Teukolsky, S.A. and Vetterling, W.T.** (1992) *Numerical Recipes In C - The Art of Scientific Computing*, Second Edition, Cambridge University Press.
- Qian, J., Ehrlich, R.W., and Campbell, J.B.** (1990) DNESYS - an expert system for automatic extraction fo drainage networks from digital elevation data, *IEEE Transactions on Geoscience and Remote Sensing*, 28(1), pp.29-45.
- Quinn, P., Beven, K., Chevallier, P. and Planchon, O.** (1991) The prediction of hillslope flow

- paths for distributed hydrological modelling using digital terrain models, *Hydrological Processes* 5, pp.59-79.
- Rees, W.G.** (1995) Characterisation and imaging of fractal topography, in **Wilkinson, G, Kanellopoulos, I. and Mégier, J.** (eds) *Fractals in Geosciences and Remote Sensing*, Joint Research Centre, Report EUR 16092 EN. pp.298-324
- Richards, K.S.** (1981) Introduction to morphometry, in **Goudie, A.S.** (ed.), *Geomorphological Techniques*, pp.25-30.
- Richardson, L.F.** (1961) The problem of contiguity: an appendix of statistics of deadly quarrels, *General Systems Yearbook*, 6, pp.139-187.
- Riley, S.** (1993) The automated extraction of drainage networks from DEMs and remotely sensed images, *Unpublished MSc Thesis, University of Leicester*.
- Robinson, G.** (1993) Measuring the accuracy of Ordnance Survey digital elevation data, *Ordnance Survey Technical Report, Ordnance Survey, Southampton*.
- Rosenfeld, A. and Kak, A.** (1982). *Digital Picture Processing*. Academic Press, Orlando.
- Roy, A., Gravel, G. and Gauthier, C.** (1987) Measuring the dimension of surfaces: a review and appriusal of different methods, *Proceedings, 8th International Symposium on Computer Assisted Cartography, Baltimore, Maryland, (Auto-Carto 8)*, pp.68-77.
- Saupe, D.** (1988) Algorithms for random fractals, pp.71-133, in **Peitgen, H.O. and Saupe, D.** (1988) (eds) *The Science of Fractal Images*, London: Springer-Verlag.
- Schalkoff, R.J.** (1989) *Digital Image Processing and Computer Vision*, London: Wiley and Sons.
- Schertzer, D. and Lovejoy, S.** (1995) Standard and advanced multifractal techniques in remote sensing, in, **Wilkinson, G, Kanellopoulos, I. and Mégier, J.** (eds) *Fractals in Geosciences and Remote Sensing*, Joint Research Centre, Report EUR 16092 EN. pp.11-40.
- Schumm, S.A.** (1956) Evolution of drainage systems and slopes in badlands at Perth Amboy, New Jersey, *Bulletin, Geological Society of America*, 67(5), pp.597-646.
- SDTS** (1990) *The Spatial Data Transfer Standard*. US Government Printing Office, US Geological Survey Bulletin, Washington DC.
- Seemuller, W.W.** (1989) The extraction of ordered vector drainage networks from elevation data, *Computer Vision, Graphics and Image Processing*, 47, pp.45-48.
- Serra, J.** (1982) *Image Analysis and Mathematical Morphology*, New York: Academic Press

- Shapiro, M. and Westervelt, J.** (1992) *r.mapcalc: An algebra for GIS and Image Processing*, US Army Construction Engineering Research Laboratory, Champaign IL.
- Shreve, R. L.** (1966). Statistical law of stream numbers. *Journal of Geology*. 74, 17-37.
- Shreve, R. L.** (1974). Variation of mainstream length with basin area in river networks. *Water Resources Research*. 10, pp.1167-1177.
- Skidmore, A.K.** (1989) A comparison of techniques for calculating gradient and aspect from a gridded digital elevation model. *International Journal of Geographical Information Systems*, 3(4), pp. 323-334
- Skidmore, A. K.** (1990). Terrain position as mapped from a gridded digital elevation model. *International Journal of Geographical Information Systems* 4(1), pp.33-49.
- Slaymaker, H.O. (ed)** (1968) Morphometric analysis of maps, *British Geomorphological Research Group, Occasional Paper*.
- Smith, G.H.** (1935) The relative relief of Ohio: *Geographical Review*, 25(2), pp.272-284
- Smith, T.R., Zhan, C. and Gao, P.** (1990) A knowledge-based two-step procedure for extracting channel networks from noisy DEM data, *Computers and Geosciences* 16(6), pp.777-786.
- Snow, R.S. and Mayer, L. (eds)** (1993) Fractals in geomorphology, *Geomorphology* 5 (1/2) (*Special Issue*)
- Speight, J. G.** (1968). Parametric description of landform. in *Land Evaluation (G. A. Stewart Ed.)*, *Proceedings of the CSIRO/UNESCO symposium, Canberra* 26-31, pp.239-250.
- Speight, J.G.** (1973). A parametric approach to landform regions, *Institute of British Geographers Special Publication 7: Progress in Geomorphology*, pp.213-230.
- Speight, J.G.** (1976). Numerical classification of landform elements from air photo data, *Zeitschrift fur Geomorphologie*, pp.154-168.
- Srinivasan, R. and Engel, B.A.** (1991) Effect of slope prediction methods on slope and erosion estimates, *Applied Engineering in Agriculture*, 7 (6), pp.779-783.
- STDs** (1990) *The Spatial Data Transfer Standard*, US Government Printing Office, Washington DC: USGS Bulletin.
- Steinhaus, H.** (1954) Length, shape and area, *Colloquium Mathematicum* 3, pp.1-13.
- Steinhaus, H.** (1960) *Mathematical Snapshots*, London: Oxford University Press.
- Stephenson, G.** (1973) *Mathematical Methods for Science Students*, London: Longman.

- Strahler, A.N.** (1964) Quantitative geomorphology of drainage basins and channel networks, in **Chow, V.** (ed) *Handbook of Applied Hydrology*, NY: McGraw-Hill, pp.39-76
- Struve, H.** (1977) *An Automated Procedure for Slope Map Construction, Final Report on project 4A152121A896*, US Army Engineer Waterways Experiment Station, Vicksburg, Miss.
- Tamura, H., Mori, S., and Yamawaki, T.** (1978) Textural features corresponding to visual perception. *IEEE Transactions on Systems, Man, and Cybernetics*. 8 (6) pp.460-473.
- Tang, L.** (1992) Automatic extraction of specific geomorphological elements from contours, *Proceedings, 5th International Symposium on Spatial Data Handling, Charleston, SC. Vol 2*, pp.554-566.
- Tarboton, D.G., Bras, R.L., and Rodriques-Iturbe, I.** (1991) On the extraction of channel networks from digital elevation data, *Hydrological Processes*, 5, pp.81-100.
- Thompson, D.W** (1917) *On Growth and Form*, Cambridge: Cambridge University Press.
- Tobler, W.R.** (1969) An analysis of a digitized surface in **Davis, C.M. (ed)** *A Study of the Land Type, Report DA-31-124-ARO-D-456*, pp.59-76, Department of Geography, University of Michigan.
- Tomita, F., Shirai, Y., Tsuji, S.** (1982) Description of texture by structural analysis, *IEEE Transactions on Pattern Analysis and Machine Intelligence*, 4(2), pp.183-191.
- Tomlin C.** (1989) *Geographic Information Systems and Cartographic Modelling*.
- Tribe, A.** (1990). Towards the automated recognition of landforms (valley heads) from digital elevation models. *Proceedings of the 4th International Symposium on Spatial Data Handling, 1990, Zurich, Switzerland*. 1, pp.45-52.
- Tricart, J.** (1947) Sur quelques indices geomorphometriques, *Comptes Rendues hebdomadaires des Seances de l'Academie des Sciences (Paris)*, 255, pp.747-749.
- Tufte, E.R.** (1990) *Envisioning Information*, Cheshire, CN: Graphics Press.
- USGS** (1987) *Digital Elevation Models Data Users Guide*. Technical Instructions, Data Users Guide 5, National Mapping Program, United States Geological Survey, Reston, VA.
- Unwin, D.J.** (1975) Introduction to trend surface analysis, *Concepts and Techniques in Modern Geography (CATMOG)* 5 pp.40. Norwich:Geobooks.
- Unwin, D.J.** (1989) Fractals in the geosciences, *Computers and Geosciences*, 15(2) pp.163-165.

- Unwin, D.J. and Wrigley, N.** (1987) Towards a general theory of control point distribution effects in trend-surface models, *Computers and Geosciences Vol 13 (4)*, pp.351-355
- Venig-Meinesz, F.A.** (1951) A remarkable feature of the Earth's topography, *Proceedings, K. Ned Akad, Wet Ser B Phys Sci, 54*, pp.212-228.
- Voss, R.F.** (1985) Random fractal forgeries, in **Earnshaw, R.A. (ed)**, *Fundamental Algorithms in Computer Graphics*, NATO ASI Series, F17, New York: Springer-Verlag, pp.805-835,
- Voss, R.F.** (1988) Fractals in nature: From characterisation to simulation, in **Peitgen, H. and Saupe D.** (eds) *The Science of Fractal Images*, London: Springer-Verlag, pp.21-70.
- Walsh, S.J., Lightfoot, D.R., and Butler, D.R.** (1987) Recognition and assessment of error in geographic information systems. *Photogrammetric Engineering and Remote Sensing*. 53, pp.1423-1430.
- Warntz, W.** (1966). The topology of socio-economic terrain and spatial flows. *Papers of the Regional Science Association*. 17, pp.47-61.
- Wartenberg, D.** (1985) Multivariate spatial correlation: A method for exploring geographical analysis, *Geographical Analysis*, 17(4), pp.263-283.
- Weibel, R. and Heller, M.** (1990). A framework for digital terrain modelling, *4th International Symposium on Spatial Data Handling*, Zurich, pp.219-229
- Weibel, R. and Heller, M.** (1991). *Digital Terrain Modelling*. in: **Maguire, D. J., Goodchild, M. F., and Rhind, D. W.** (eds.) *Geographical Information Systems: Principles and Applications*, pp.269-297, Longman, London.
- Werner, C.** (1988) Formal analysis of ridge and channel patterns in maturely eroded terrain. *Annals of the Association of American Geographers*, 78 (2), pp. 253-270.
- Weszka, J, Dyer, C., Rosenfeld, A.** (1976) A comparative study of texture measures for terrain classification, *IEEE Transactions on Systems, Man and Cybernetics*, 6(4), pp.269-285.
- Wilkinson, G, Kanellopoulos, I. and Mégier, J.** (1995) (eds) *Fractals in Geosciences and Remote Sensing*, Joint Research Centre, Report EUR 16092 EN.
- Wolf, G.W.** (1984). A mathematical model of cartographic generalization. *Geo-Processing 2*, pp.271-286.
- Wolf, G.W.** (1989). Data structures for the topological characterisation of topographic surfaces. *Paper presented at the Sixth European Colloquium of Theoretical and Quantitative Geography, Chantilly, France*.

- Wolf, G.W.** (1991) A Fortran subroutine for cartographic generalisation, *Computers and Geosciences*, 17(10), pp.1359-1281.
- Wood, J.D.** (1990a). Automated surface feature detection from digital elevation data. Part one: a review and classification. *Midlands Regional Research Report no. 20*.
- Wood, J.D.** (1990b) Automated surface feature detection from digital elevation data. Part two: Implementation. *Midlands Regional Research Laboratory Research Report no. 21*.
- Wood J.D. (1993)** Measuring and reporting the accuracy of Ordnance Survey digital elevation data, *Ordnance Survey Technical Report, Ordnance Survey, Southampton*.
- Wood, J.D. (1995)** Scale-based characterisation of Digital Elevation Models, *Proceedings, 3rd National Conference on GIS Research UK (GISRUK '95), Newcastle*.
- Wood J. and Fisher P. (1993)** Assessing interpolation accuracy in elevation models, *IEEE Computer Graphics and Applications*, 13 (2), pp.48-56.
- Wood, J., Unwin, D., Stynes, K., Fisher, P. and Dykes, J.** (1996) The use of the landscape metaphor in understanding spatial data, *Environment and Planning B, (in press)*.
- Wood, W.F. and Snell J.B.** (1957) The dispersion of geomorphic data around measures of central tendency and its application, *US Army Quartermaster Research and Development Center, Research Study Report EA-8*.
- Wood, W.F. and Snell J.B.** (1960) A Quantitative system for classifying landforms, *US Army Quartermaster Research and Development Center, Technical Report EP-124*.
- Young, M. (1978)** Terrain analysis: program documentation. *Statistical Characterisation of altitude matrices by computer: Report 5 on grant DA-ERO-591-73-G0040*, University of Durham, England.
- Yuan, L. P. and Vanderpool N. L.** (1986). Drainage network simulation. *Computers and Geosciences* 12 (5), pp.653-665.
- Yoeli, P.** (1967) Mechanisation in analytical hill-shading. *Cartographic Journal* 4, pp.82-88
- Yoeli, P.** (1984) Computer assisted determination of the valley and ridge lines of digital terrain models, *International Yearbook of Cartography*, 24, pp.197-206.
- Yoeli, P.** (1986) Computer executed production of a regular grid of height points from digital contours, *The American Cartographer* 13(3), pp.219-229
- Yokoya, N., Yamamoto, N. and Funakubo, N.** (1989) Fractal-based analysis and interpolation of 3D natural surface shapes and their application to terrain modelling, *Computer*

Vision, Graphics and Image Processing, 46, pp.284-302

Zevenbergen, L.W. and Thorne, C.R. (1987) Quantitative analysis of land surface topography. *Earth Surface Processes and Landforms* 12, pp.47-56.

Zhang, M.C., Campbell, J.B. and Haralick, R.M. (1990). Automatic delineation of drainage basins within digital elevation data using the topographic primal sketch. *Mathematical Geology* 22 (2), pp.189-209.